Development of small organic fluorescent probe for glutathione detection

Dissertation submitted to
Visvesvaraya National Institute of Technology, Nagpur
in partial fulfilment of the requirements for the award of
the degree

Master of Science
in
Chemistry

by

Riya Upadhyay
(MS23CHM020)

under the guidance of

Prof. Sujit Kumar Ghosh

Department of Chemistry

Visvesvaraya National Institute of Technology

Nagpur 440010 (India)

May 2025

Development of small organic fluorescent probe for glutathione detection

Dissertation submitted to
Visvesvaraya National Institute of Technology, Nagpur
in partial fulfilment of the requirements for the award of
the degree

Master of Science
in
Chemistry

by

Riya Upadhyay
(MS23CHM020)

under the guidance of

Prof. Sujit Kumar Ghosh

Department of Chemistry

Visvesvaraya National Institute of Technology

Nagpur 440010 (India)

May 2025

© Visvesvaraya National Institute of Technology (VNIT) 2009

Department of Chemistry
Visvesvaraya National Institute of Technology

Declaration

I, **Riya Upadhyay**, hereby declare that this dissertation titled **"Development of small organic fluorescent probe for glutathione detection"** is carried out by me in the Department of **Chemistry** of Visvesvaraya National Institute of Technology, Nagpur. The work is original and has not been submitted earlier whole or in part for the award of any degree/diploma at this or any other Institution / University.

Riya Upadhyay
(MS23CHM020)
Date:13.05.25

Certificate

This to certify that the dissertation titled **"Development of small organic fluorescent probe for glutathione detection"** is submitted by **Riya Upadhyay** in partial fulfilment of the requirements for the award of the degree of **Master of Science in Chemistry**, VNIT Nagpur. The work is comprehensive, complete and fit for final evaluation.

VISVESVARAYA NATIONAL INSTITUTE OF TECHNOLOGY, NAGPUR

Non-Plagiarism Certificate

Certified that M. Sc. dissertation titled **"*Development of small organic fluorescent probe for glutathione detection*"** submitted by **Riya Upadhyay,** Enrolment no. **MS23CHM020,** ID No. **30715** has been examined for plagiarism using TURNITIN software, and the overlap is within acceptable limits. An overview of the report is provided below;

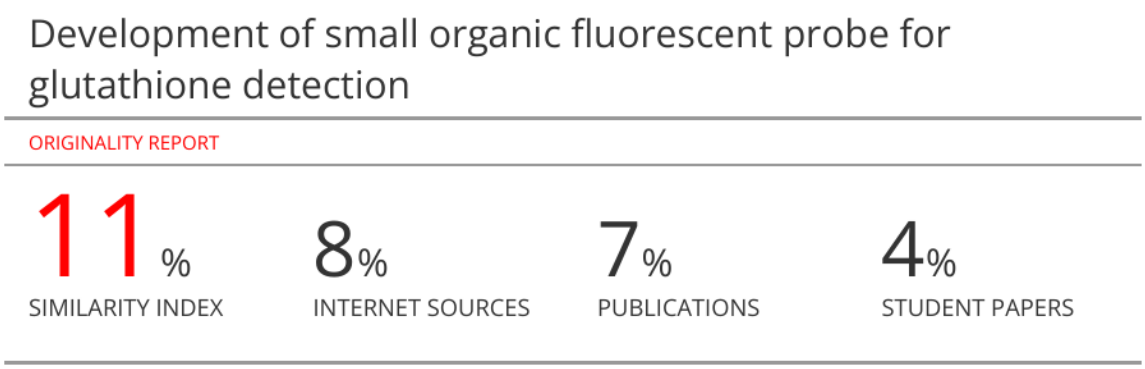

Acknowledgement

My sincere gratitude goes out to the Almighty for giving me the courage to make my endeavor a success. Professor Sujit Kumar Ghosh, my project supervisor, has my sincere gratitude for his knowledgeable direction and unwavering support during this process. He encouraged me to push above my own boundaries and aim for nothing less than excellence with his insightful feedbacks and unwavering support. The loving and constructive learning atmosphere he established, together with his unfailing faith in my talents, was critical to the project's success.

Additionally, I would like to thank Dr. Abhishek Banerjee, the Assistant Professor in the Chemistry Department, and his group of Ph.D. students for their invaluable support during the IR studies.

Everyone in the Photochemistry and Biophysical Spectroscopy Laboratory deserves my heartfelt gratitude, including Mrs. Aditi Garg, Mr. Piyush Singh, Ms. Shrestha Banerjee, Mr. Subham Chattopadhyay, Mr. Subham Das, and Mr. Puneet Mishra. Their enthusiastic conversations, unwavering collaboration, and teamwork enhanced our work and enabled us to overcome numerous obstacles. This team's unique perspectives and unwavering dedication were critical to meeting our objectives.

Lastly, I would like to thank Ms. Yashika Pradhan for her support and help. I would want to express my sincere gratitude to my parents and my brother for their unwavering encouragement, affection, and concern during this effort. Their belief in me, together with the sacrifices they made and the understanding they offered throughout long working hours, provided the tenacity required to overcome difficult circumstances. Without their unwavering support this achievement would have been impossible.

DEDICATED TO MY PARENTS

MRS. RASHMI UPADHYAY

AND

MR. SACHCHIDA NAND UPADHYAY

Abstract:

Cancer is a disease characterized by uncontrolled growth of cells. It has major challenge of late diagnosis, which is one of the main reasons behind death. Due to oxidative stress, a disbalance occur between free radicals and antioxidants. Cancer cells exhibit higher concentration of glutathione (GSH), compared to normal cells, potentially as a mechanism to cope with increased oxidative stress. The aim and objective of this research work is to examine the capability of the small, highly sensitive and selective organic fluorescent probe in detection of GSH. The thesis encompasses the details of synthesis of a novel naphthalimide based fluorescent probe 3-((4-chlorobenzylidene) amino)-N-phenyl-1,8 naphthalimide (3C-NAPH). In the process of probe synthesis, a fluorescent precursor 3-amino-N-phenyl-1,8-naphthalimide (3A-NAPH) has been synthesized and its photophysical properties have been studied including steady-state absorption and emission, excited-state dynamics and solvent mixture studies. Quantum chemical calculations have been conducted to attain further understandings over solvatochromic behavior of 3A-NAPH and 3C-NAPH. The key aspect of this research work involves inspecting the interaction and selectivity of the developed probe 3C-NAPH with GSH. To examine such interaction, the concentration dependent study of 3C-NAPH has been scrupulously analyzed and found that the probe is sensitive and selective towards GSH. Limit of detection has been found out to be 6.53uM. Therefore, suggested mechanism involves a nucleophilic substitution reaction between the thiol group of GSH and the Cl group of the probe. This results in modifications in the probe's electronic structure and thus quenching in its fluorescence intensity. Considering the high levels of GSH in cancer cells, a capable probe could offer a quick and cost-effective approach for early cancer diagnosis, ultimately leading to earlier treatment intervention and improved survival chances for patients.

Keywords: Cancer, Glutathione (GSH), Naphthalimide, Photophysical properties, Quantum chemical calculations, Solvatochromic behavior, Nucleophilic substitution reaction, Quenching

List of Figures

Fig. 1 Cancer as a metabolic disorder 3
Fig. 2 Glutathione 5
Fig. 3 Jablonski diagram 7
Fig. 4 Morse potential energy profile for electronic transitions. 8
Fig. 5 The Beer-Lambert law 18
Fig. 6 The double beam spectrophotometer 19
Fig. 7 Representation of spectrofluorometer 21
Fig. 8 Electronics module of TCSPC 23
Fig. 9 Computational results of 3A-NAPH 26
Fig. 10 Computational results of 3C-NAPH 27
Fig. 11 Computational results after 3C-NAPH binded with GSH 27
Fig. 12 Synthetic route of 3C-NAPH 28
Fig. 13 IR spectra of 3N-NAPH 29
Fig. 14 IR spectra of 3A-NAPH 30
Fig. 15 IR spectra of 3C-NAPH 30
Fig. 16 Absorption spectra of 3A-NAPH in different solvent system 32
Fig. 17 Emission spectra of 3A-NAPH in different solvent system 33
Fig. 18 Lifetime of 3A-NAPH in different solvent system 34
Fig. 19 Lifetime(ns) VS Polarity plot of 3A-NAPH 34
Fig. 20 Absorption spectra of 3A-NAPH in solvent mixture system 35
Fig. 21 Emission spectra of 3A-NAPH in solvent mixture system 36
Fig. 22 Emission Intensity VS % Glycerol plot of 3A-NAPH 37
Fig. 23 Lifetime of 3A-NAPH in solvent mixture system 38
Fig. 24 Lifetime(ns) VS % Glycerol plot of 3A-NAPH 38
Fig. 25 Emission spectra of 3C-NAPH with different solvent system 39
Fig. 26 Emission spectra of 3C-NAPH in different concentration of GSH 40
Fig. 27 Plot of emission intensity of 3C-NAPH with different concentration of GSH 41
Fig. 28 Emission spectra of different concentration of 3C-NAPH with GSH 42
Fig. 29 Plot of emission intensity of different concentration of 3C-NAPH with GSH 42
Fig. 30 Absorption spectra of 3C-NAPH with different amino acid and bio-thiol 43
Fig. 31 Emission spectra of 3C-NAPH with different amino acid and bio-thiol 44
Fig. 32 Emission spectra of 3C-NAPH with amino acid and bio-thiol 45
Fig. 33 Plot of emission intensity vs with different amino acid and bio-thiol 45
Fig. 34 Diagram to show on-off mechanism of the probe 45

Abbreviations

GSH: Glutathione

IC: internal conversions

IRF: instrument response function ISC: intersystem cross

TCSPC: time-correlated single photon counting

ICT: Intramolecular charge transfer

CT: Charge transfer

LE: Locally excited

TRF: time-resolved fluorescence

VR: vibrational relaxations

GS: Ground State

ES: Excited state

DCM: Dichloromethane

ACN: Acetonitrile

$CHCl_3$: Chloroform

EtOH: Ethanol

DFT: Density Functional Theory

HOMO: Highest Occupied Molecular Orbital

LUMO: Lowest Unoccupied Molecular Orbital

Index

1 INTRODUCTION 2

1.1 Motivation of the work 2

1.2 Cancer as a metabolic disorder 2

1.3 Glutathione and its role in cancer cell 4

1.4 Glutathione detection methods 5

1.5 Introduction to Photophysics 6

1.5.1 Absorption 7

1.5.2 Franck-Condon Principle 7

1.5.3 Emission Pathways 9

1.5.4 Solvatochromism 11

1.6 Aim and Objective of this work 13

2 RESOURCES AND ADVANCES 16

2.1 Materials and chemicals 16

2.2 Sample preparations 16

2.3 UV-Visible spectrophotometer 16

2.4 Spectrofluorometer 19

2.5 Time Resolved Fluorescence Measurements 21

3 DESIGN, SYNTHESIS AND CHARACTERIZATION 25

3.1 Theoretical calculations 25

3.2 Experimental studies 25

3.2.1 Materials 25

3.2.2 Instrumentation 26

3.3 Synthetic route and characterizations 26

3.3.1 Theoretical calculations results 26

3.3.2 Synthesis of Probe 28

3.3.3 Structural confirmation of synthesized molecule 29

4 PHOTOPHYSICAL ANALYSIS 32

4.1 Solvatochromism study of 3A-NAPH 32
4.1.1 Electronic absorption study 32
4.1.2 Steady state emission study 33
4.1.3 Excited state dynamics study 34
4.2 Solvent Mixture Study of 3A-NAPH 35
4.2.1 Solvent mixture absorption study 35
4.2.2 Solvent mixture emission study 36
4.2.3 Excited state dynamics study of solvent mixture 37
4.3 Solvatochromism study of 3C-NAPH 38
4.3.1 Electronic emission study 39
4.4 Concentration dependent study of 3C-NAPH 39
4.4.1 Emission study of probe with GSH with varying concentration of GSH 40
4.4.2 Limit of detection 41
4.4.3 Emission study of probe with GSH with varying concentration of probe 41
4.5 Amino acid dependent study of 3C-NAPH 42
4.5.1 Selectivity study of probe 43
4.5.2 Competitive study of the probe 44
5 CONCLUSION AND PROSPECTS 47
5.1 Conclusion 47
5.2 Future scope 47
6 REFERENCES 49

CHAPTER 1

INTRODUCTION

1 INTRODUCTION

1.1 Motivation of the work

According to World Health Organization estimates for 2022, cancer killed 9.7 million people[1]. Normal cells develop and follow the concept of contact inhibition, however malignant cells lose this ability, allowing them to continue growing and forming tumors.[2] Not all tumors are cancerous; those that stay in their original site are known as benign tumors. Malignant tumors, on the contrary, invade cells nearby and grow through the body, often via the circulation. Metastasis, which usually happens in the fourth stage of cancer, is the term used to describe this spread from the initial site to other places. As a result, late detection can delay treatment, making cancer the second greatest cause of death. Delays in diagnosis can result in a 10–20% reduction in survival rates. Therefore, early diagnosis is essential for the treatment of cancer.

Age, genetic predisposition, smoking, obesity, alcohol use, UV light exposure, and exposure to radiation are all factors that contribute to cancer. Therefore, early diagnosis is essential for the treatment of cancer. Age, smoking, obesity, genetic predisposition, alcohol use, UV light exposure, and radiation are all risk factors for developing cancer. According to research, tumor suppressor genes or proto-oncogenes may be mutated to cause cancer. Cancer cells have higher concentrations of GSH (2-10 millimolar) than normal cells (0.2-5 micromolar).[3,4] Consequently, a promising avenue for cancer screening may arise if GSH is identified early.

1.2 Cancer as a metabolic disorder

According to research, tumor suppressor genes or proto-oncogenes may be mutated to cause cancer.[2] Nonetheless, metabolic abnormalities or alterations are routinely noted in a variety of cancer forms. Therefore, using a metabolic approach to treat cancer may work. An experiment

was carried out to confirm this, demonstrating the important part that cellular cytoplasm plays in the development of cancer. Researchers saw different outcomes when they switched the nuclei of normal cells with mitochondrial DNA (mt DNA) abnormalities and malignant cells.[2]

When a normal nucleus was inserted into a malignant cytoplasm, the cells that emerged formed tumors despite lacking the genomic alterations that are generally associated with cancers.[2] When a malignant nucleus was put in normal cytoplasm, the cells did not form tumors, despite retaining cancer-related genomic aberrations. This emphasizes how important the cellular environment—especially the cytoplasm—is in determining how cells behave, underscoring its importance in the study of cancer and possible therapies. This implies that cytoplasmic activities within cells have a role in the genesis of cancer.[2]

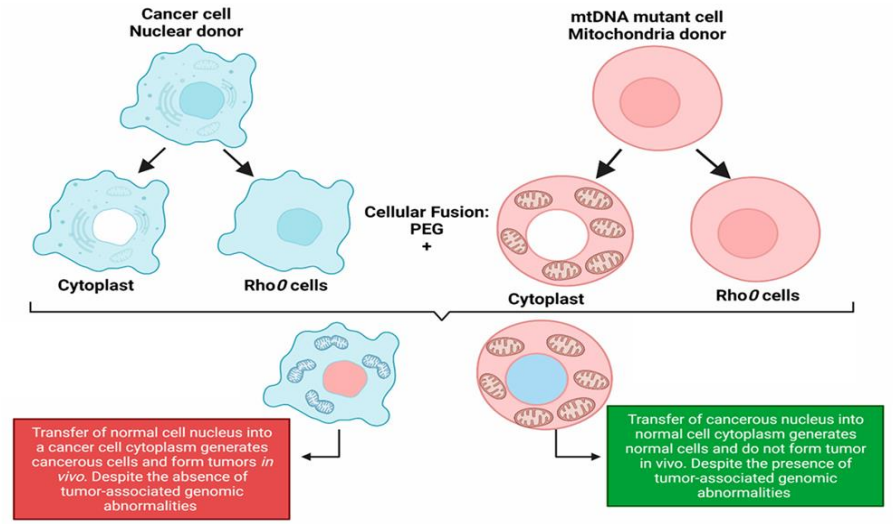
Cancer cell
Nuclear donor
mtDNA mutant cell
Mitochondria donor
Cellular Fusion:
PEG
+
Cytoplast
Rho0 cells
Cytoplast
Rho0 cells
Transfer of normal cell nucleus into a cancer cell cytoplasm generates cancerous cells and form tumors in vivo. Despite the absence of tumor-associated genomic abnormalities
Transfer of cancerous nucleus into normal cell cytoplasm generates normal cells and do not form tumor in vivo. Despite the presence of tumor-associated genomic abnormalities

Fig. 1 Cancer as a metabolic disorder

Animal cells have mitochondria, which are distinguished by their membrane. The electron transport chain, which makes up the majority of ATP—32 ATP molecules—is found in the inner membrane.[2] Glycolysis in the cytoplasm produces two ATP, while the Krebs cycle in the mitochondrial matrix produces two ATP through substrate-level phosphorylation.[4] This process produces the remaining ATP. 32 ATP is produced by oxidative phosphorylation.[2] However, in cancer cells, the

inner membrane of the mitochondria, or even the entire mitochondria, might be destroyed, inhibiting phosphorylation. As a result, cancer cells must rely completely on glycolysis for ATP synthesis, causing them to consume huge amounts of glucose (also known carboholics). This phenomenon was first identified by Warburg and is known as the Warburg effect.[2]

1.3 Glutathione and its role in cancer cell

One bio-thiol that is present in the body is GSH.[5] A tripeptide made up of glutamic acid, cysteine, and glycine is called glutathione (GSH).[6] Glutamic acid forms a gamma-peptic bond with cysteine through its gamma-glutamyl group. There are two types of GSH: the reduced form (GSH), which makes up the bulk of GSH and reaches millimolar concentrations in the intracellular compartment, and the oxidized form (GSSG), which accounts for less than 1% of total GSH.[6] The majority of GSH is located intracellularly (approximately 90%), with mitochondria accounting for roughly 10% and the endoplasmic reticulum accounting for a very minor percentage.[6]

Mitochondria are primarily harmed by oxidative stress, which occurs when the quantity of free radicals in the cell exceeds that of antioxidants.[7] Factors including radiation, poisons, and viruses increase this stress by generating reactive oxygen species during cellular respiration in the electron transport chain, which results in the creation of free radicals.[8] These free radicals seek stability by grabbing electrons from biomolecules, which triggers a chain reaction that causes biomolecular damage. To protect itself from these free radicals, the body uses antioxidants.[9] Antioxidants neutralize free radicals, but they also become free radicals. These antioxidants work together, with other antioxidants giving electrons to destroy newly produced antioxidant free radicals.[10] There are four categories of antioxidants: first-, second-, third-, and fourth-line defense antioxidants.[11]

The first-line defense stops free radicals from forming and acts before they are generated.[12] Second-line defense operates after the production

of free radicals to neutralize them.[10] After free radicals have been neutralized, third-line defense antioxidants counteract the harm that free radicals have produced.[13] Antioxidants that fight free radicals are crucial for second-line defense. Ascorbic acid, uric acid, and glutathione are the second-line antioxidants [13,10].

Ascorbic acid and uric acid can operate as both prooxidants and antioxidants depending on their concentrations, while glutathione is an antioxidant that neutralizes a wide range of oxidants and is prevalent in the human body [1011] . Compared to normal cells (0.2–5 micromolar), cancer cells have a greater glutathione content (2–10 millimolar).[14] Due to mitochondrial damage, cancer cells undergo a transformation into primitive, anaerobic cells, which results in elevated GSH levels.[7] Cancer cells cannot use oxygen and hence produce glutathione to avoid poisoning since they do not want to come in contact with oxygen. As a result, metabolite screening aids in early detection and pre-cancer screening while remaining quick and cost-effective.

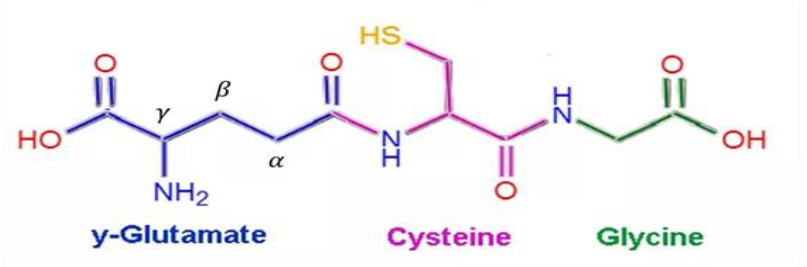

Fig. 2 Glutathione

1.4 Glutathione detection methods

Capillary electrophoresis, chromatography, flow cytometry, electrochemical techniques, and nuclear magnetic resonance are all ways for detecting GSH levels.[15] These methods, however, are frequently pricy, intricate, and inappropriate for real-time monitoring in biological systems. High sensitivity, specificity, cost-effectiveness, and real-time detection are some benefits of fluorescence probes, particularly organic ones.[15]

Inorganic fluorescent probes have limitations in biological contexts, whereas organic probes are preferred for their low detection limits, ease of synthesis, clinical relevance, and biocompatibility.[16] The goal was to create a highly selective organic fluorescent probe for GSH detection, specifically in cancer cell imaging. Biological detection has made use of a number of fluorophores, such as coumarin, benzothiazole, rhodamine, and naphthalimide.[16]

Naphthalimide is unique because of its exceptional biocompatibility, great photostability, resistance to photobleaching, synthetic flexibility, and bright fluorescence.[17] Because of its significant Stokes shift, which reduces interference, it is perfect for imaging applications.[18] It is essential to biochemical research, especially when it comes to identifying glutathione, a vital antioxidant that is involved in cellular functions.[19]

1.5 Introduction to Photophysics

Photophysics investigates the mechanisms that occur when molecules absorb light while retaining their chemical structure. When a molecule absorbs a given wavelength, it undergoes photoexcitation, which raises its electronic state. Because these excited states are unstable, the molecule loses the excess energy—either by creating light through radiative processes or by converting the energy into heat through nonradiative means—and eventually returns to its ground state. Professor Alexander Jablonski designed the Jablonski diagram, which clearly explains these complex processes inside a basic framework. Molecular spectroscopy studies the absorption and emission of light by molecules. According to the Maxwell-Boltzmann distribution, the majority of molecules are at ambient temperature and occupy their lowest vibrational state. Significant thermal energy increases in a system are mainly used to increase rotational and vibrational motions rather than to induce electronic transitions. Pyrolysis, or molecular dissociation, can occur if this internal energy gain is significant enough to cause bond rupture. But if the frequency of EMR matches

the frequency of molecule, it is being absorbed.

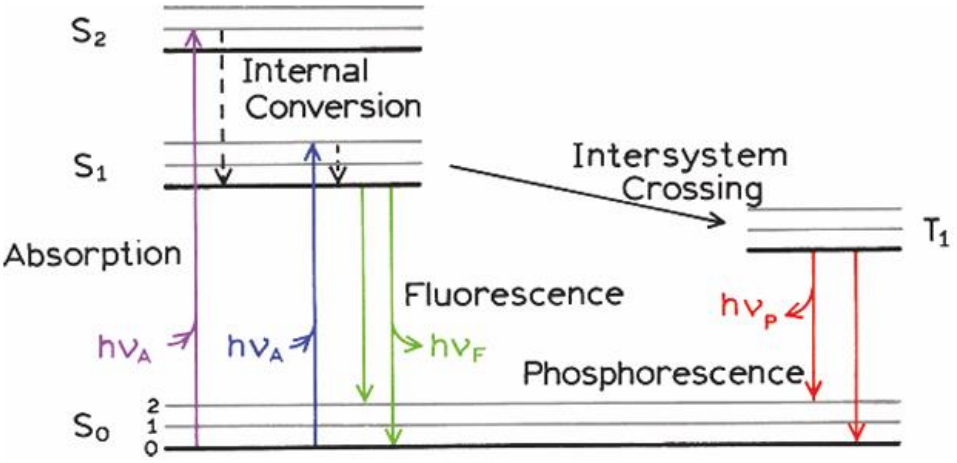

Fig. 3 Jablonski diagram

1.5.1 Absorption

Absorbance is the process where a molecule absorbs UV-Vis electromagnetic radiation. This occurs when the frequency of radiation and that of molecule (natural frequency) matches. This lead photon to be absorbed, promoting molecule to a higher energy level. The phenomenon is quantitatively described by the Beer–Lambert law, Lambert's law states that *when a single-wavelength light beam passes through a homogeneous medium containing an absorbing substance, the amount of light absorbed or decrease in intensity of light is determined by both the concentration (c) of the absorbing species and the distance (l) traveled through the medium.*[20] It can be written as-

$$\frac{-\mathrm{d}I}{I} \alpha \; C \,.dl \cdot \mathrm{d}l$$

1.5.2 Franck-Condon Principle

According to the Franck-Condon principle, electronic transitions occur so swiftly in relation to nuclear mobility that the nuclei remain

nearly fixed throughout the procedure.[20] As a result, the most intense absorption features appear when the vibrational wavefunctions of the ground and excited states overlap optimally, which is known as the most probable transition. This is visually represented by a vertical line on the Morse potential energy curve, indicating that the nuclear coordinates remain constant during electronic excitation.[21]

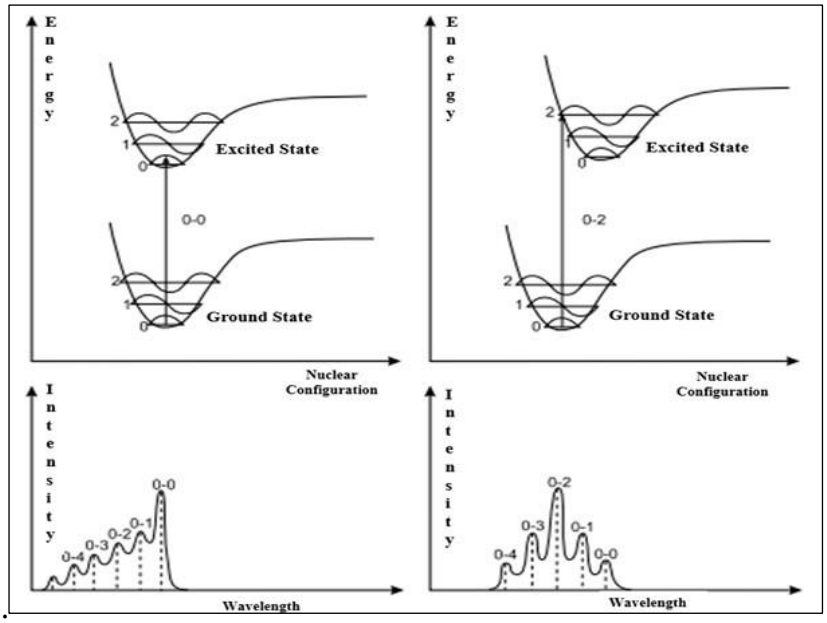

Fig. 4 Morse potential energy profile for electronic transitions.

Light absorption by molecules can lead to two types of excited states. In a singlet state, electrons are paired (S = 0, multiplicity 1), but in a triplet state, electrons are unpaired. Hund's rule prefers electron configurations with parallel spins; hence the triplet state is frequently more stable than the singlet form. Under typical conditions, only transitions between singlet states are permitted; however, spin selection requirements prohibit transitions from a singlet to a triplet state. However, factors such as spin-orbit coupling can lower these limitations, allowing previously inconceivable transitions to occur. The link between electronic structure and selection rules is crucial for comprehending various photophysical processes and material reactions to different

radiation circumstances.

1.5.3 Emission Pathways

When molecules are electronically excited, they release surplus energy using a variety of relaxation methods. These may be radiative (emitting light) or non-radiative. The Franck-Condon principle governs these emission events in the same way that it governs absorption; the most likely transitions are those in which the vibrational wavefunctions of the excited and ground states overlap the most, as determined by nuclear position. In low-pressure conditions with few collisions, an excited molecule can return to its ground state by emitting light with the same wavelength it absorbed, a phenomenon known as resonance radiation.[20] To summarize, emission processes are classified into radiative and non-radiative channels.

1.5.3.1 Non-radiative photophysical pathways

Nonradiative decay happens when surplus energy is released without emitting photons, and the energy is often transformed into thermal energy or passed to the surrounding environment. In Jablonski diagram non-radiative pathways are represented by a wavy arrow. Important nonradiative routes include:

- **Internal conversion**

When an excited molecule undergoes internal conversion, it quickly and non-radiatively comes to a lower electronic state within the same spin multiplicity (for example, from S_2 to S_1 or S_1 to S_0) without releasing a photon. Rather, vibrational motions lose surplus energy, which is then released as heat. This process, which is typically represented on a Jablonski diagram as a curved line connecting vibrational levels in various electronic states, can be accelerated by collisions with solvent molecules. The short timescale (varying from 10^{-13} to 10^{-11} seconds for transitions from

highly excited states to S_1 and around 10^{-8} seconds for S_1 to S_0 transitions) implies it competes aggressively with fluorescence, affecting the total quantum yield of light emission.

- **Intersystem crossing**

An excited molecule can move between states with various spin multiplicities, usually from a singlet state (S_1) to a triplet state (T_1), through a nonradiative process called intersystem crossing (ISC). Under normal circumstances, spin conservation makes this transition "spin-forbidden," but spin-orbit coupling, which allows states with different spins to mix, makes ISC possible. The singlet and triplet states are connected by a curved arrow on a Jablonski diagram; these phenomena are shown in this way.[21] This usually happens in picoseconds to a few nanoseconds. Once the molecule has reached the triplet state, it may undergo additional nonradiative relaxation processes or eventually become phosphorescent.

1.5.3.2 Radiative photophysical pathways

Radiative emission is associated with the release of energy in the form of photons. It is shown with straight arrow in Jablonski diagram. The primary radiative pathways include-

- **Fluorescence**

Fluorescence is a quick radiative process in which an excited molecule releases light before returning to its ground state. This process happens incredibly quickly i.e. 10^{-9} s. When a molecule absorbs a photon, one electron is excited from the ground state (S_0) to the first excited singlet state (S_1) very instantly, according to the Franck-Condon principle. This means that the nuclei remain nearly constant during this excitation. No matter what excited state a molecule enters after absorbing light, Kasha's rule states that it will rapidly relax to the lowest excited singlet state (S_1) through nonradiative mechanisms (such as internal conversion) before

emitting any light. As a result, the fluorescence we see is always caused by the $S_1 \rightarrow S_0$ transition, which means the emission spectrum is largely independent of the initial excitation wavelength. Since some energy is lost during relaxation, the emitted light has a lower energy (and thus a longer wavelength) than the absorbed light—a phenomenon known as the Stokes shift.[20] Fluorescence's efficiency is assessed by its quantum yield, which indicates the balance of radiative and nonradiative processes.

- **Phosphorescence**

When a molecule absorbs light, it is usually stimulated into a singlet form. In some situations, the molecule can move from an excited singlet state to a triplet state (T_1) through intersystem crossing, which is nonradiative. This triplet state has unpaired electrons with parallel spins, making the direct transition to the singlet ground state (S_0) radiatively prohibited by spin selection criteria. As a result, the return to the ground state is very slow and energy is released as light on a significantly longer timescale—ranging from microseconds to several seconds or more. The lengthy duration of phosphorescence is mostly caused by this inefficient radiative transition from the triplet state.

- **Delayed Fluorescence**

Delayed fluorescence occurs when a molecule initially crosses over into a triplet state and then converts back to a singlet state using a reverse intersystem crossing mechanism. Thermal energy assisted transition from triplet to singlet states. Once the molecule has returned to the singlet state, it emits light in the same way as it does in fluorescence. The essential distinction is that this fluorescence occurs after a delay caused by time spent in the triplet state.

1.5.4 Solvatochromism

The polarity of the solvent affects a molecule's absorption or

emission wavelength, changing the chromophore's electronic environment.[22] This effect can be divided into two types: positive solvatochromism, where an increase in solvent polarity generates a red shift (longer wavelengths), and negative solvatochromism, where an increase in polarity causes a blue shift (shorter wavelengths).[22] The mechanism underlying this shift is mostly determined by interactions between a molecule's ground and excited states, with a more polar excited state stabilizing in polar solvents, resulting in a red shift.[23] Additionally, charge transfer effects can influence spectral shifts because polar liquids improve charge separation. Another aspect is Twisted Intramolecular Charge Transfer (TICT), which occurs when donor-acceptor systems undergo molecular twisting in polar settings, diminishing fluorescence intensity while changing emission wavelengths.

1.5.4.1 Charge transfer (CT) states

Charge transfer (CT) states are formed when electrical stimulation redistributes charge within a molecule or between donor-acceptor pairs, influencing absorption and emission spectra in fluorescent and optoelectronic materials. Electrons move from the donor (D) to the acceptor (A) during CT absorption, frequently displaying weaker oscillator strengths than π-π^* transitions.[23] Solvent polarity is important because stronger polarity stabilizes the CT state, resulting in a red shift, whereas non-polar solvents cause a blue shift.[23,24] The larger CT absorption bands can overlap with typical π-π^* transitions, making spectral interpretation more difficult.[24]

1.5.4.2 Locally Excited (LE) states

Locally excited (LE) states occur when an electron changes from the ground state to an excited state within the same molecule, without considerable charge redistribution.[24] They are frequently found in organic fluorophores, conjugated systems, and π-π transitions in aromatic compounds. In LE absorption, an electron

transfers from the highest occupied molecular orbital (HOMO) to the lowest unoccupied molecular orbital (LUMO), usually by π-π transitions. This results in crisp and well-defined absorption bands with high oscillator strengths and significant light absorption. Unlike charge transfer (CT) states, LE states have limited dependency on solvent polarity, with only minor shifts caused by solvent relaxation.[24] In LE fluorescence, the excited electron relaxes back to its ground state, resulting in high quantum efficiency and brilliant emissions with a slight Stokes shift caused by vibrational relaxation and solvent interactions.[24] Because charge separation is small in LE states, their emission spectra are relatively unaffected by solvent polarity, making them ideal for bioimaging, optoelectronics, and molecular probes.[23]

1.6 Aim and Objective of this work

The results of this study are intended to show that the proposed naphthalimide-based fluorescent probe has the capacity to detect GSH selectively. Given the elevated levels of GSH in cancer cells, a successful probe could provide a rapid and cost-effective method for early cancer diagnosis and pre-cancer screening, ultimately leading to earlier therapeutic intervention and improved patient survival rates.

- Designing of organic fluorescent probe based on nucleophilic substitution approach.
- Synthesis of organic fluorescent probe through condensation and reduction followed by Schiff base formation approach and elucidating the structure by various spectroscopic techniques.
- To ascertains photophysical characteristics of molecule, electronic absorption and steady state emission is recorded.
- To explore characteristics in different solvent system, solvatochromic study with different solvents

with varying polarity and proticity of solvents.

- Quantum Chemical Calculations of Designed Probe.
- Identification and Interpretation of quenching of probe intensity with GSH.
- Identification and Interpretation of selectivity of probe with GSH over other amino acids.

CHAPTER 2

RESOURCES AND ADVANCES

2 RESOURCES AND ADVANCES

This chapter covers several spectroscopic inspection techniques and materials, including sample preparations. Methods include fluorescence lifetime measurements by time resolved fluorescence (TRF) using time correlated single photon counting (TCSPC), steady state fluorescence by spectrofluorometer, and UV-VIS absorption by spectrophotometer.

2.1 Materials and chemicals

Trifluoroacetic acid (TFA), 4-chlorobenzaldehyde, 1,4-dioxane, 3-nitro-1,8-naphthalimic anhydride, and other chemicals were obtained from Sigma-Aldrich in India and used without purification. Merck, India, provided the stannous chloride ($SnCl_2$), which was utilized exactly as directed. Fischer-Scientific in India provided spectroscopic-grade solvents such as ethanol, toluene, THF, ethyl acetate, petroleum ether, DMSO, $CHCl_3$, DCM, and acetonitrile. Always, Millipore water—which came from a Millipore filtration system—was utilized. To ensure reproducibility, every experiment was conducted thrice.

2.2 Sample preparations

Spectroscopic grade dioxane and dimethylformamide (DMSO) were used to create stock solutions of 3A-NAPH and 3C-NAPH, respectively, at a concentration of 1 mM for spectroscopic investigations. The thesis presented in this context employs a variety of standard spectroscopic techniques, the basic concepts of which are discussed in the following sections.

2.3 UV-Visible spectrophotometer

A UV-Visible spectrophotometer is an important analytical

equipment for measuring the absorbance or transmittance of light through a sample, which aids in determining the physicochemical properties of a variety of substances such as metal ions, organic compounds, biomolecules, and pharmaceutical drugs. It measures the difference between incident and transmitted light at wavelengths ranging from 190 to 1100 nm, providing insights into molecular interactions.

The Beer-Lambert Law, which describes how a substance's concentration and the thickness of the medium effect light absorption, is the foundation of this technique. According to Lambert's Law, which was developed in 1760, the intensity of monochromatic light diminishes exponentially as it travels through a substance, emphasizing the function of chromophores in absorbing particular light wavelengths. Lambert's Law is written as:

$$\mathbf{\ln(I_0/I_t) = Kl}$$

Beer's Law, established in 1859, describes how light absorption is proportional to the concentration of absorbing molecules in a sample. By explaining how a monochromatic light beam becomes less intense when it comes into contact with more absorbing species, it enhances Lambert's Law. In this equation, I_0 represents the incident light intensity, I_t represents the transmitted light intensity, and l refers to the sample's path length, usually 1 cm. This theory is crucial in spectroscopy, allowing researchers to calculate material concentrations using their absorbance. Beer's Law is written as:

$$\mathbf{\ln(I_0/I_t) = Kc}$$

In this equation, c is the concentration in moles per litre.

The Beer-Lambert Law combines Beer's and Lambert's principles, saying that the intensity of a monochromatic light beam drops as it travels through a transparent material containing an absorbing substance. This drop is determined by both the concentration of the

absorbing species and the thickness of the medium. Before transmission, the light may be altered by absorption, reflection, interference, and scattering, all of which influence the measured intensity. Beer-Lambert Law is expressed as:

$$\ln(I_0/I_t) \propto lc$$

Also,

$$\log(I_0/I_t) = \varepsilon . l . c$$

ε represents the proportionality constant (molar absorptivity or molar extinction coefficient), whose unit is expressed in litres per mole per centimeter (L mol-1 cm-1). There is a relation:

$$A = -\log T$$

Here, A= absorbance and T = transmittance. Spectrophotometer actually measure the % of transmittance light from the sample.

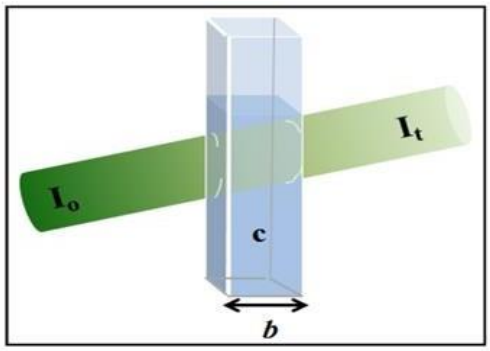

Fig. 5 The Beer-Lambert law

There are various types of spectrophotometers, such as split-beam, double-beam, and single-beam models. Blank and sample are measured independently by single-beam spectrophotometers, which might result in inaccuracies because of differences in lamp intensity. Double-beam spectrophotometers address this issue by splitting the light beam, resulting in uniform intensity readings in both blank and sample cuvettes. The JASCO V-630 double-beam UV-visible spectrophotometer operates at 298K, using a deuterium lamp (190-

350 nm) for UV light and a halogen lamp (330-1100 nm) for visible light. Using a diffraction grating, a monochromator, and mirrors, the device selects particular wavelengths of light. A beam splitter then separates the light into two paths—one for the sample and one for the reference—allowing the detector to precisely quantify intensity differences and optimize spectral analysis.

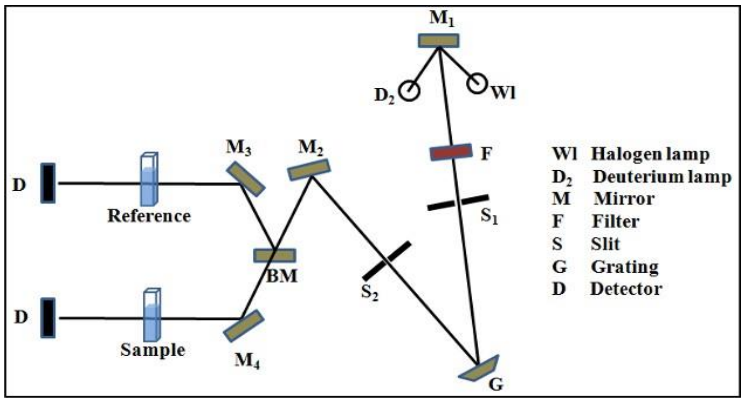

Fig. 6 The double beam spectrophotometer

2.4 Spectrofluorometer

A vital technique in scientific and medical research, fluorescence spectroscopy is used in molecular biology, biophysics, biochemistry, clinical diagnostics, and environmental studies. It is prized for its accuracy, quickness, and sensitivity. A fluorophore absorbs light at a given wavelength before emitting it at a slightly longer wavelength when it returns to its ground state. Spectrofluorometers evaluate this emission to determine the properties of various fluorophores based on their excitation and emission wavelengths.[21]

A JASCO FP-8300 spectrofluorometer was utilized to capture steady-state emission, excitation, and phosphorescence spectra. To ensure precision, the measurements were taken with a 1.0 cm quartz cell with a 2.5 nm slit width. The excitation source was a xenon lamp because of its high intensity and wide wavelength range,

which began at 250 nm. Mirrors M1 and M0 directed the lamp's light to the excitation monochromator's entrance slit S1, where diffraction grating G1 dispersed the light to guarantee that only monochromatic wavelengths entered the exit slit. The excitation monochromator employs two gratings to reduce stray light, and holographic concave gratings further reduce undesired signals. Half of the monochromatic light is directed to a silicon photodiode (PD) for monitoring by a beam splitter (BS), while the remaining portion enters the sample compartment by mirrors M3 and M4 and focuses on the sample cell. The emitted fluorescence then travels to slit S2 of the emission monochromator via mirrors M5, M6, and M7. Last but not least, the PMT detector records the light intensity and transforms it into a proportionate electrical current for examination. The PMT can detect individual photons, which can then be analyzed as an average signal or counted separately.

The spectrofluorometer records both excitation and emission spectra, with the emission spectrum representing fluorescence intensity at a fixed excitation wavelength and the excitation spectrum reflecting intensity variations at a fixed emission wavelength. Shutters, a magnetic stirrer, and filter holders provide for precise control in the sample chamber. In contrast to shutters, which exclude undesirable light, polarizers aid in the analysis of fluorescence anisotropy and the selective detection of polarized excitation or emission components.[21]

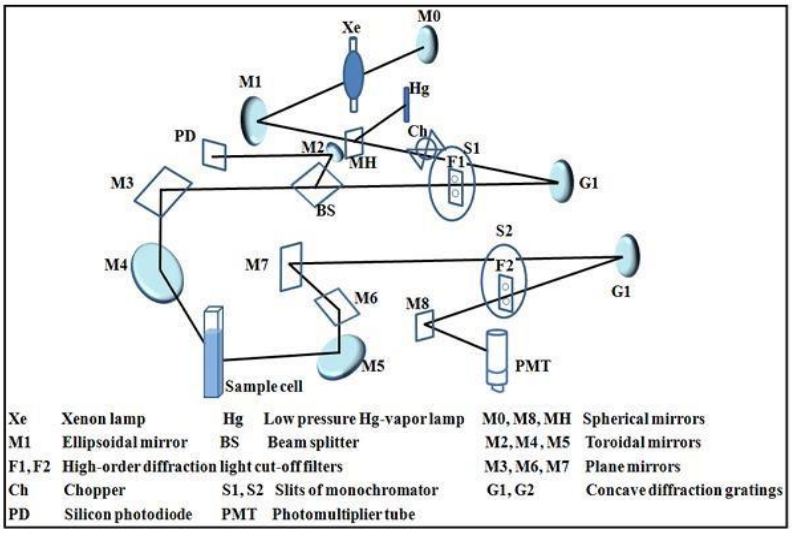

Fig. 7 Representation of spectrofluorometer

2.5 Time Resolved Fluorescence Measurements

Time-resolved fluorescence measurement is crucial for studying excited-state dynamics in various scientific fields. It helps analyze photophysical, photochemical, and photobiological processes by tracking emitted light intensity over time. There are three main fluorescence lifetime measurement techniques: Stroboscopic Technique (Strobe) & Time-Correlated Single Photon Counting (TCSPC) - Both operate in the time domain, measuring fluorescence decay after pulsed excitation. This study used Time-Correlated Single Photon Counting (TCSPC) to determine the excited-state lifetime of the fluorophore by analyzing fluorescence decay curves over time.[21] To ensure accuracy, both the fluorescence decay and the instrument response function (excitation pulse) were measured, as the finite width of the LED or LASER pulse can distort the sample's true fluorescence response. Fluorescence lifetime measurements were conducted using Time-Correlated Single Photon Counting (TCSPC) with a picosecond diode-driven driver and 280/340 nm excitation source, integrated into a PTI time-resolved spectrofluorometer (USA). The PTI light-emitting diode had a pulse width of 700-1100 ps, while the PMD-2 detector

featured a 180 ps response time and 813 fs temporal resolution. The detector covered an emission spectral range of 185-820 nm and was designed. At 340/280 nm (±10 nm), the fluorescence instrument response was measured using SDS, a Rayleigh scatterer with a bandwidth of 2.5 nm. Felix GX software (version 4.1.2) was employed to gather and examine data. The decreased χ^2 criterion and the fitted function's unpredictability in comparison to the raw data were used to evaluate the correctness of the exponential fits.

The average fluorescence lifetime (<τ>) for 3A-NAPH decay was calculated utilizing the individual decay periods (τi) and their respective contributions (αi) using a mathematical equation.

$$\langle\tau\rangle = \sum \tau_i \alpha_i / \sum \alpha_i$$

Time-Correlated Single Photon Counting (TCSPC) detects single photons and logs their arrival times following excitation in order to calculate the fluorescence lifetime. It works like a stopwatch, with the START pulse beginning with a light signal and the STOP pulse ending when a fluorescence photon is detected.

The signals' time difference is recorded in a histogram, which plots time on the X-axis and divides it into tiny intervals (Δt). Each detected signal is assigned to a bin, the width of which determines measurement accuracy. This histogram helps with lifespan studies by offering a thorough profile of fluorescence intensity over time.[21]

The TCSPC instrument employs specialized electronics to determine the timing difference between single-photon pulses from a detector and reference pulses from a lamp control device or a second detector. The excitation pulse from a LASER or LED excites the sample and transmits signals to the system. Constant Fraction Discriminators (CFD) filter out low pulses and trigger at a predetermined fraction of pulse height for both reference and photon pulses. This method minimizes timing jitter, resulting in more exact fluorescence lifetime measurements.

When a single photon pulse is detected, the Time-to-Amplitude Converter (TAC) generates a voltage that grows linearly over nanoseconds until another reference pulse is received. Each LED light pulse produces a new reference signal even when no photons are detected. In order to guarantee precision, the reference signal is postponed coinciding with the photon pulse from the same cycle. A Constant Fraction Discriminator (CFD) calculates the exact arrival time and stops the voltage ramp. The TAC generates a voltage based on the time delay (Δt) between excitation and emission, which is amplified by a Programmable Gain Amplifier (PGA) for further processing.

By converting the amplified voltage signal into a digital value, the Analog-to-Digital Converter (ADC) allocates it to a corresponding memory location. The signal is limited to a particular voltage range in order to avoid erroneous readings. If the signal is outside of this range, a Window Discriminator (WD) suppresses it. After storing the digital voltage, a histogram of the decay is produced by repeating this procedure with a pulsed light source.[21]

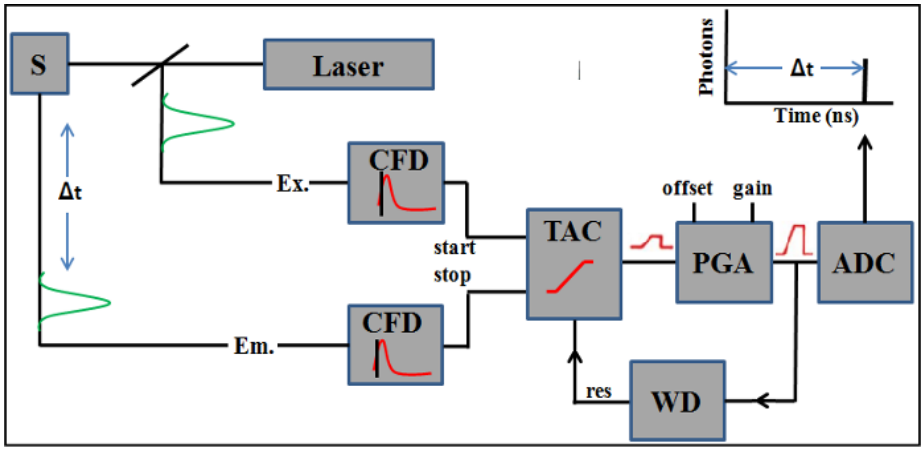

Fig. 8 Electronics module of TCSPC

CHAPTER 3

DESIGN, SYNTHESIS AND CHARACTERIZATION

3 DESIGN, SYNTHESIS AND CHARACTERIZATION

This chapter deals with design and synthesis of 3C-NAPH which is naphthalimide based moiety. The IUPAC name of the molecule is (E)-5-((4-chlorobenzylidene)amino)-2-phenyl-1H-benzo[de]isoquinoline-1,3(2H)-dione. The theoretical studies have to be done on this molecule for finding its theoretical energy diagram and theoretical absorption peak. The synthesized molecule has been characterized by infrared (IR) spectroscopy technique for further understanding about the structures.

3.1 Theoretical calculations

Density Functional Theory (DFT) with the B3LYP functional and the 6-311G basis set is used to perform the computational analysis for ground-state optimization. Excited-state properties, including vertical excitation energies for singlet and triplet states, are calculated using Time-Dependent Density Functional Theory (TD-DFT) with the B3LYP functional and the 6-311G basis set. Using the Gaussian09 software, these computations are carried out on an Intel Xeon E5504 CPU with 4 cores, 8 threads, and 13.7 GB of RAM. GaussView program is used to see the computational results and do extensive analyses.

3.2 Experimental studies

3.2.1 Materials

The following reagents were purchased from Sigma-Aldrich in India: 3-nitro-1,8-naphthalic anhydride, zinc anhydride dihydrate, Stannous Chloride, KOH, trifluoroacetic acid, Glutathione. All of these were used without purification. For experimental investigations, Spectrochem India provided HPLC-grade solvents, including petroleum ether, DCM, THF, ACN, DMSO, dioxane,

hexane, toluene, ethanol and ethyl acetate.

3.2.2 Instrumentation

3.1.1.1 FTIR study – The solid state of 3N-NAPH, 3A-NAPH and 3C-NAPH were analyzed. KBr was used as a solid immersion agent to record the infrared spectrum (400-4000 cm-1) on a Nicolet iS50 ThermoFisher Scientific spectrophotometer equipped with a DTGS detector and KBr beamsplitter assembly.

3.3 Synthetic route and characterizations

3.3.1 Theoretical calculations results

Through quantum chemical calculations of 3A-NAPH we can see a change in dipole moment from 6.147 Debye in ground state to 11.483 Debye in excited state which predict a large bathochromic shift in absorbance and emission spectra, showing charge transfer state. Also, the electron density has shifted towards acceptor part of naphthalimide in LUMO from doner amino group in HOMO.

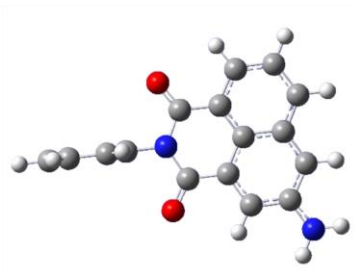

3-amino-N-phenyl-1,8-naphthalimide

Dipole Moment [E.S.]	11.483 Debye
Dipole Moment [G.S.]	6.147 Debye

Dipole Moment and Dihedral angle of Excited and Ground state

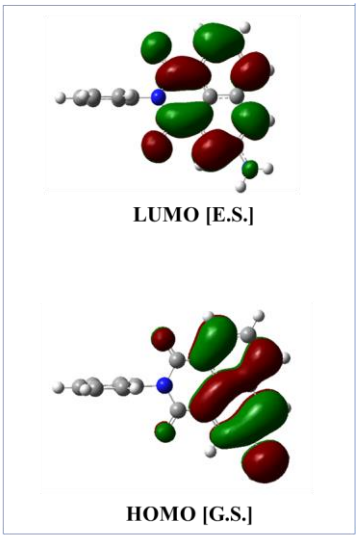

HOMO and LUMO of 3A-NAPH

Fig. 9 Computational results of 3A-NAPH

Through quantum chemical calculations of 3C-NAPH we can see a change in dipole moment from 5.4 Debye in ground state to 4.9

Debye in excited state which predict a very small or negligible shifts in absorbance and emission spectra, showing locally excited state.

Also, the electron density has shifted towards 4-chlorobenzylidene part of naphthalimide in LUMO from naphthalimide part in HOMO, suggesting potential of showing nucleophilic substitution reaction with -SH (sulfhydryl) of GSH.

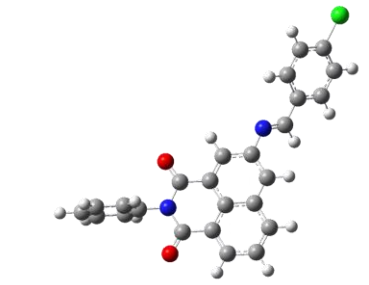

3-((4-chlorobenzylidene)amino)-N-phenyl-1,8-naphthalimide

Dipole Moment [E.S.]	4.999 Debye
Dipole Moment [G.S.]	5.468 Debye

Dipole Moment of Excited and Ground state

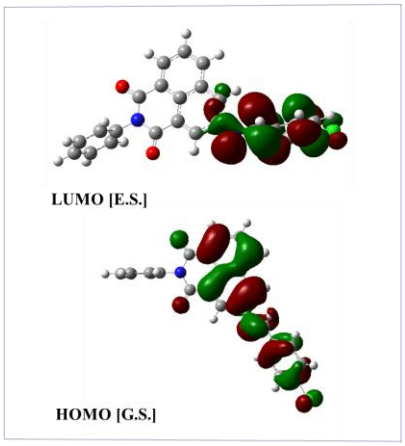

HOMO and LUMO of 3C-NAPH

Fig. 10 Computational results of 3C-NAPH

Through quantum chemical calculations of 3C-NAPH we can see a change in dipole moment from 14.2 Debye in ground state to 13.3 Debye in excited state. The electron density has shifted towards 4-chlorobenzylidene part of probe in LUMO from naphthalimide part in HOMO, suggesting similar kind of photophysical properties as that of the probe.

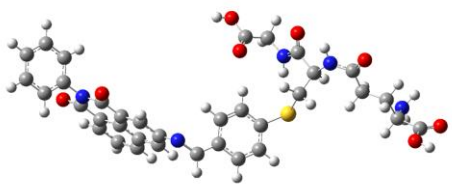

Probe with GSH

Dipole Moment [E.S.]	13.358 Debye
Dipole Moment [G.S.]	14.248 Debye

Dipole Moment of Excited and Ground state

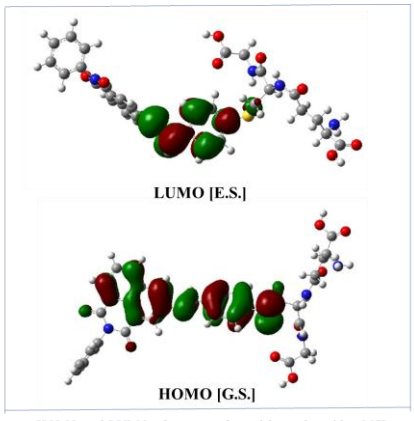

HOMO and LUMO of structure formed by probe withy GSH

Fig. 11 Computational results after 3C-NAPH binded with GSH

3.3.2 Synthesis of Probe

3-nitro-1,8-naphthalic anhydride (1 equivalent) and zinc anhydride dihydrate (1 equivalent) were thoroughly diluted in ethanol (30 mL). Next came the addition of aniline (1.1 equivalent). For 30 hours, the mixture was refluxed in a N_2 environment while being stirred. After the reaction, the liquid was cooled, filtered using Whatman filter paper, and dried. 3N-NAPH, a light brown substance, was produced using silica gel column chromatography. After dissolving 3N-NAPH (1 equivalent) and Stannous Chloride (5 equivalent) in ethanol, they interacted for three hours. Then, a workup using KOH water and ethyl acetate was carried out. Following the reaction, the solvent was concentrated and the crude product purified using silica gel column chromatography. 3A-NAPH (1 equivalent) and 4-chlorobenzaldehyde (1.2 equivalent) were dissolved in 30 mL 1,4-dioxane, then 4-5 drops of trifluoroacetic acid were added to a round-bottomed flask and refluxed for 72 hours[25] [26]. Following the reaction, the solvent was concentrated, and the crude product was purified using silica gel column chromatography, yielding a light yellow 3C-NAPH.

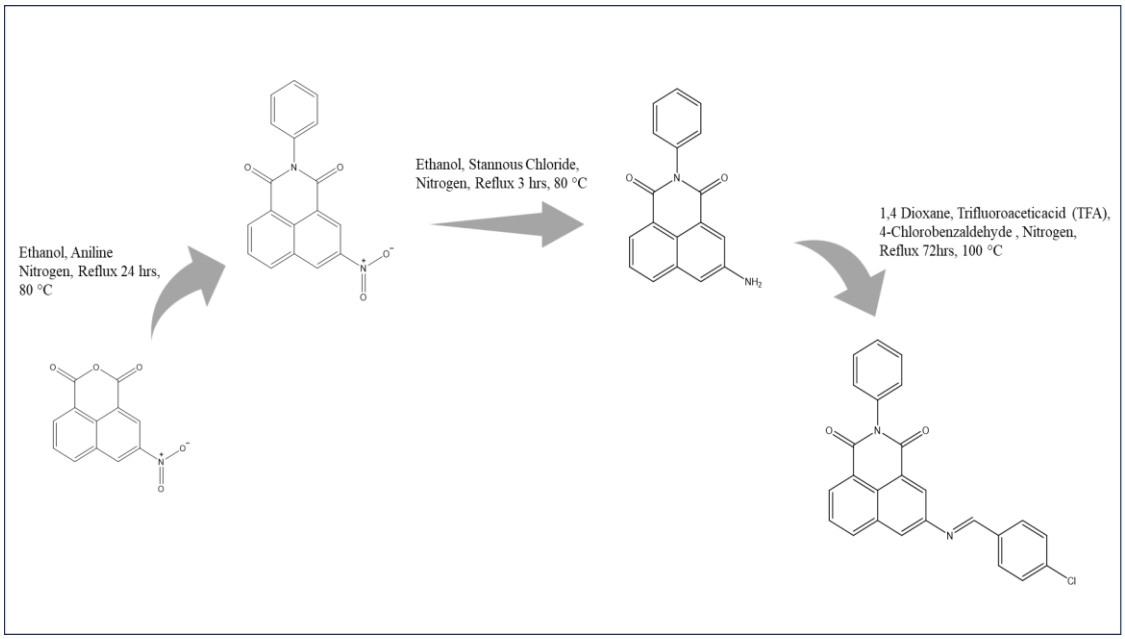

Fig. 12 Synthetic route of 3C-NAPH

3.3.3 Structural confirmation of synthesized molecule

3.3.3.1 Structural elucidation through IR spectroscopy

IR spectroscopy is typically used to identify functional groups in a chemical, giving an early indication of molecular structure but not complete confirmation. In this work, imide was expected to have peaks in the 1680-1730 cm^{-1} range. 3N-NAPH, 3A-NAPH, 3C-NAPH have this peak, but change in electron density results in three different peaks: At 1710, 1700 and 1716 cm^{-1}. Peaks at 1540 cm^{-1} and 1340 cm^{-1} in fig. 13 are linked to N=O stretching in 3N-NAPH. Peaks at 3450 cm^{-1} and 3360 cm^{-1} in fig. 14 are linked to N-H stretching in 3A-NAPH. While the peak at 1594 cm^{-1} in fig. 15 are linked to C=N stretching in 3C-NAPH. These findings offer initial evidence that the chemical might have developed.

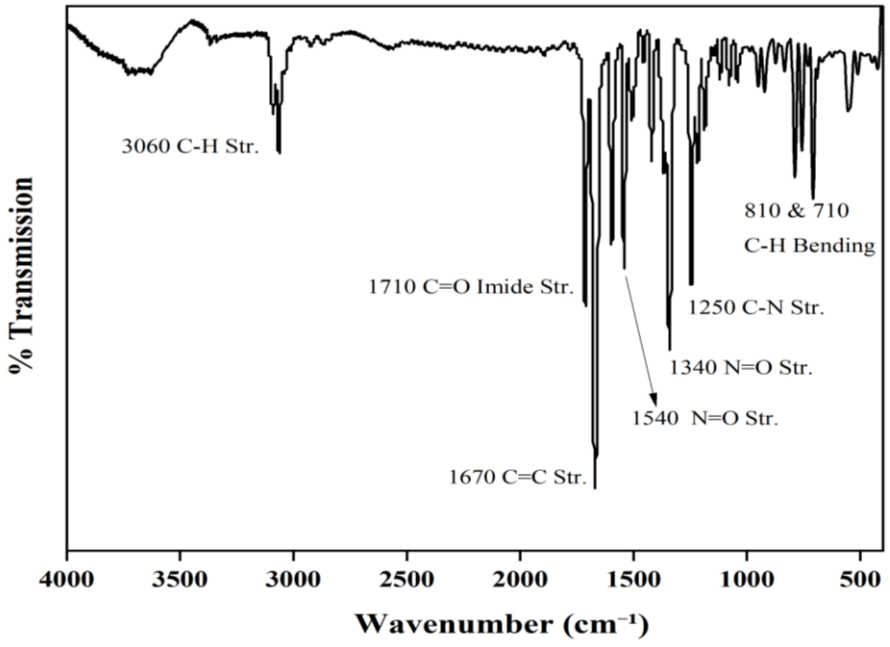

Fig. 13 IR spectra of 3N-NAPH

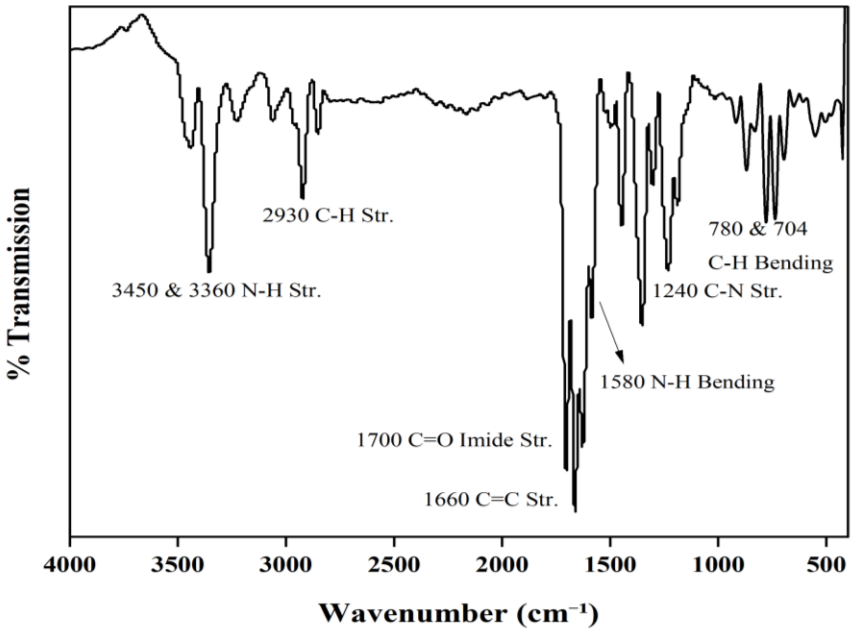

Fig. 14 IR spectra of 3A-NAPH

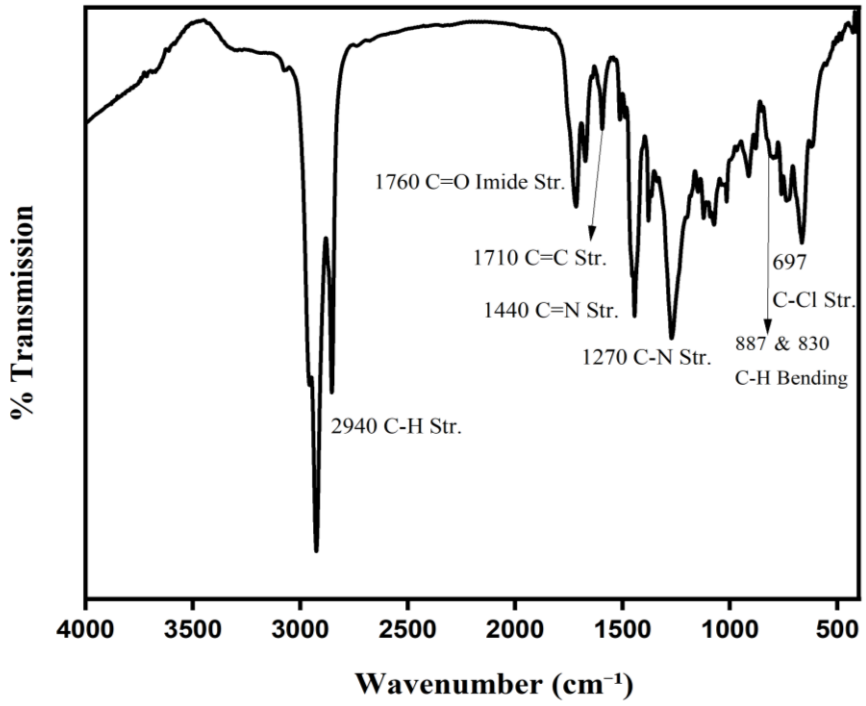

Fig. 15 IR spectra of 3C-NAPH

CHAPTER 4

PHOTOPHYSICAL ANALYSIS

4 PHOTOPHYSICAL ANALYSIS

This chapter deals with the different photophysical studies of the molecule like solvatochromism study including absorption, emission and fluorescence lifetime of the molecule in different solvent from less polar solvent to very polar solvents. All of the evidence points to our molecule's selective GSH sensing.

4.1 Solvatochromism study of 3A-NAPH

To study the solvatochromic behavior of our molecule in different solvent polarity order, we take the solvents hexane, toluene, dioxane, DCM, ACN, and ethanol. For the Solvatochromism study we make 1mM sample solution in dioxane. The results are discussed below-

4.1.1 Electronic absorption study

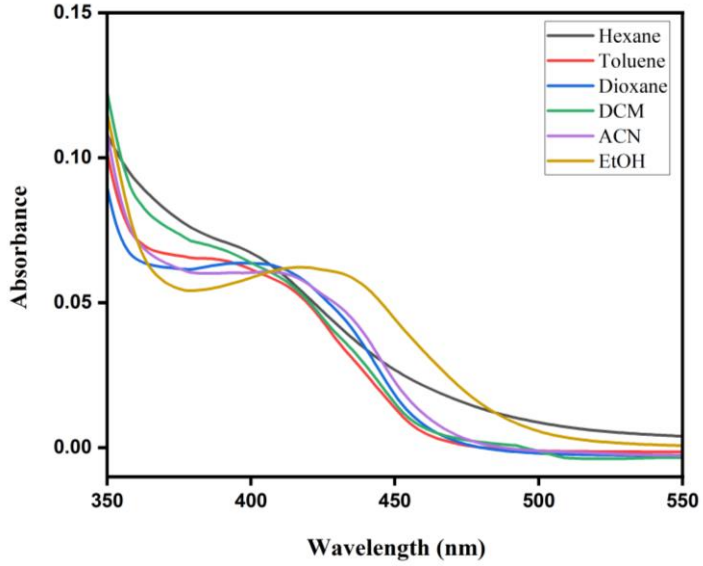

Fig. 16 Absorption spectra of 3A-NAPH in different solvent system

A careful examination of the spectra reveals that in hexane—a solvent with comparatively low polarity—the absorption maximum is observed at 402 nm. As the polarity increases, the absorption peak

shifts to 424 nm in acetonitrile (ACN) and further to 431 nm in ethanol. This shift toward longer wavelengths indicates that higher solvent polarity leads to a red shift in the absorption spectrum. The data suggest that as the solvent polarity increases from hexane to ethanol, a charge-transfer state develops. In more polar environments, a dipole moment is induced within the molecule due to electron movement from a donor to an acceptor unit, thereby stabilizing the S_1 state and resulting in the observed red-shifted spectra.[23,24] According to quantum chemical calculations we can see a change in dipole moment from 6.147 Debye in ground state to 11.483 Debye in excited state (refer fig.9), which also confirms the bathochromic shift of absorbance spectra.

4.1.2 Steady state emission study

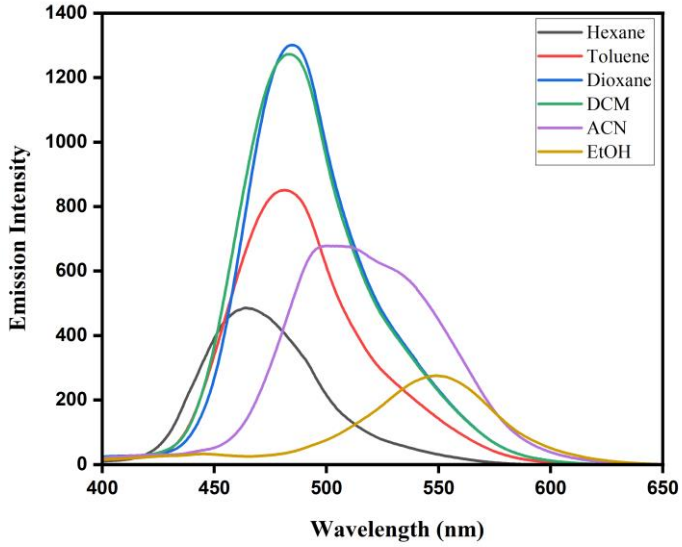

Fig. 17 Emission spectra of 3A-NAPH in different solvent system

The emission spectra reveal that in hexane—a solvent with low polarity—the emission maximum is found at 464 nm (in arbitrary units). As the solvent polarity increases, a red shift is observed in dioxane the maximum moves to 484 nm, in ethanol it shifts further to 551 nm, though the intensity drops to 205. This red shift indicates that with higher polarity, a charge-transfer state is being developed,

which stabilizes the S_1 state—a trend that aligns well with the red-shift in absorption data.[23] Interestingly, the emission intensity increases with solvent polarity up to dioxane, after which it begins to decline. This suggests that in solvents of intermediate polarity, the charge-transfer character enhances the emission, but in even more polar environments, the formation of a twisted intramolecular charge transfer (TICT) state becomes significant. To examine the presence of TICT state solvent mixture study has been conducted and analyzed in the next section of this chapter.

4.1.3 Excited state dynamics study

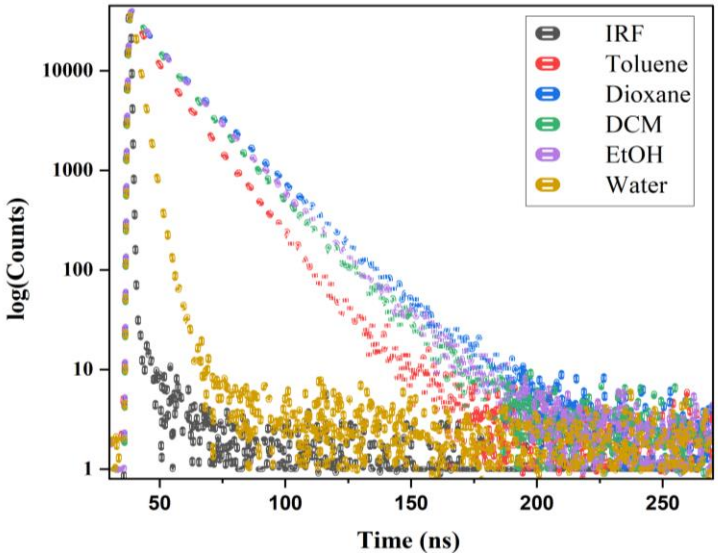

Fig. 18 Lifetime of 3A-NAPH in different solvent system

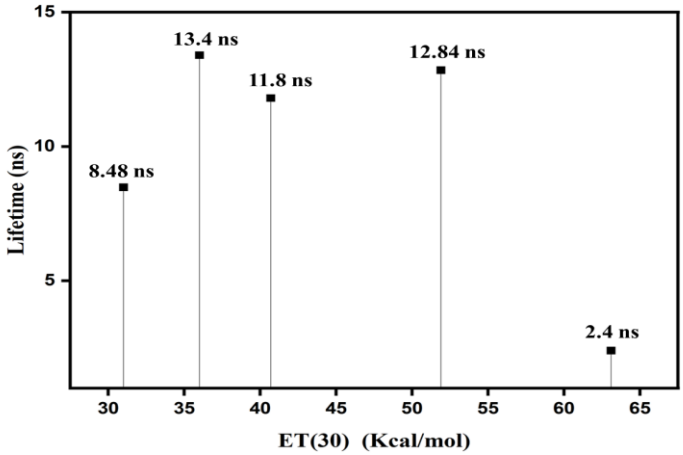

Fig. 19 Lifetime(ns) VS Polarity plot of 3A-NAPH

Fluorescence lifetime is the average time a fluorescent molecule spends in its excited state before emitting a photon and returning to its ground state. This lifetime is measured using Time-Correlated Single Photon Counting (TCSPC), which aids in the analysis of fluorescence emission timing. We observe that in the dioxane lifetime is highest. From the lifetime exponential decay curve, we can see very less fluorescence lifetime in case of water near to IRF value. Here, IRF stands for Instrument Response Function in this context. The IRF is the temporal profile of the system's reaction to a single light pulse.

4.2 Solvent Mixture Study of 3A-NAPH

To analyze the TICT behavior of our molecule in polar solvents, we conducted a solvent mixture study in Ethanol and Glycerol mixture. For this study we made 1mM sample solution of 3A-NAPH in dioxane. The results are discussed below-

4.2.1 Solvent mixture absorption study

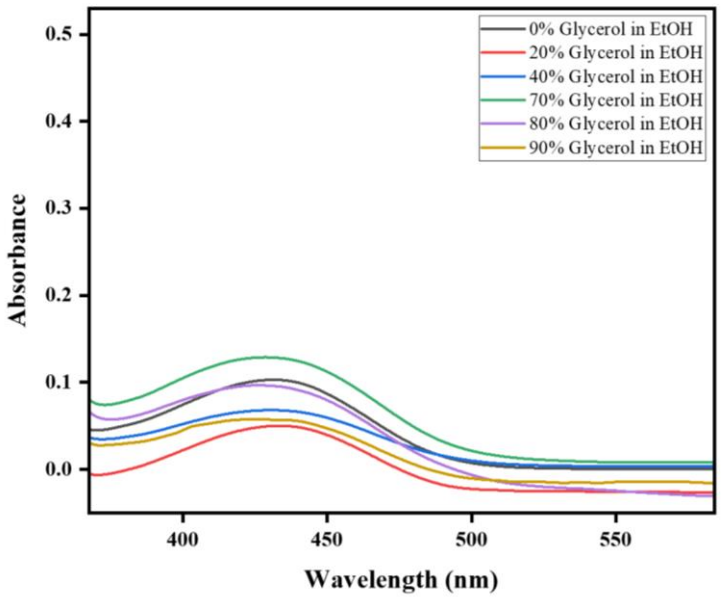

Fig. 20 Absorption spectra of 3A-NAPH in solvent mixture system

A scrupulous examination of the absorbance spectra reveals that there is no significant change in wavelength with increase in viscosity. In 0% glycerol in ethanol the absorption maximum is observed at 435 nm. As the viscosity increases, the absorption peak shifts from 435 to 432 nm in 90% glycerol in ethanol. This negligible red shift leads to a conclusion that TICT could be present as it is an excited state phenomena and there are no significant changes observed in ground state as we can see in absorption spectrum. Therefore, emission spectra have been observed.

4.2.2 Solvent mixture emission study

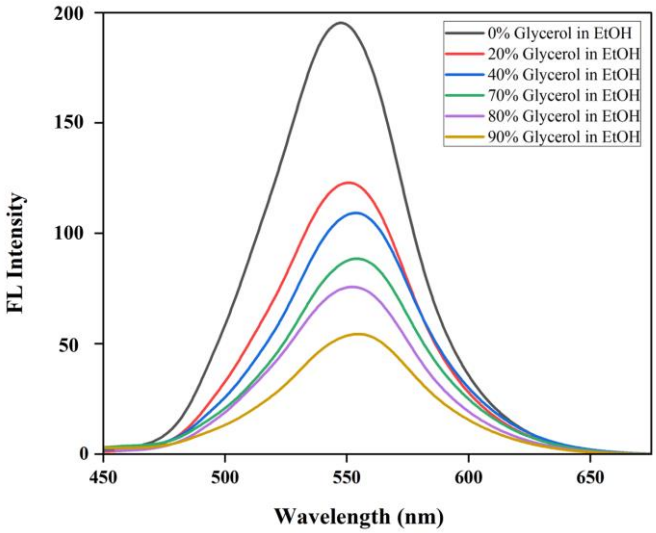

Fig. 21 Emission spectra of 3A-NAPH in solvent mixture system

The emission spectra reveal that with increase in viscosity due to glycerol in ethanol mixture the emission maximum show a red shift from 547nm in 0% glycerol in ethanol to 555nm in 90% glycerol in ethanol (in arbitrary units). As the mixture viscosity increases, a decrease in intensity is observed, which is contrast of the result that we have been expecting in case of TICT. We were expecting an increase in the emission intensity as fluorescence intensity in Twisted Intramolecular Charge Transfer (TICT) increases with viscosity due to restricted molecular mobility. Higher viscosity prevents molecules from twisting into nonradiative states, so

keeping them in the locally excited state and increasing fluorescence. Additionally, it restricts solvent relaxation, which lowers energy loss and maintains emission. Since we have observed a decrease in intensity, we can say TICT is not present in the molecule. To examine the presence of TICT state solvent mixture excited state dynamic study has been conducted and analyzed.

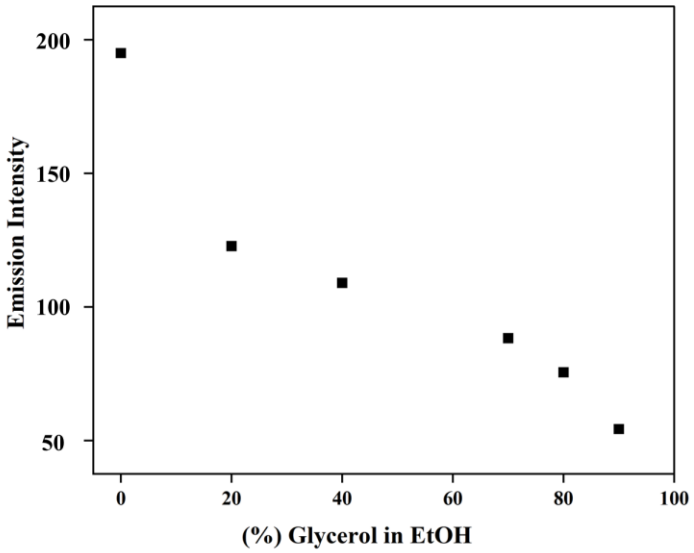

Fig. 22 Emission Intensity VS % Glycerol plot of 3A-NAPH

4.2.3 Excited state dynamics study of solvent mixture

We have observed that as there is an increase in viscosity the life time decreases, which was expected to increase as increase in glycerol concentration increases the viscosity restricts the movement of the molecule resulting in the increase in average life time of the molecule. In case of 100% glycerol, from the lifetime exponential decay curve, we can see very less fluorescence lifetime near to IRF value. With decrease in intensity and life time data we can conclude the absence of TICT state in polar solvents.

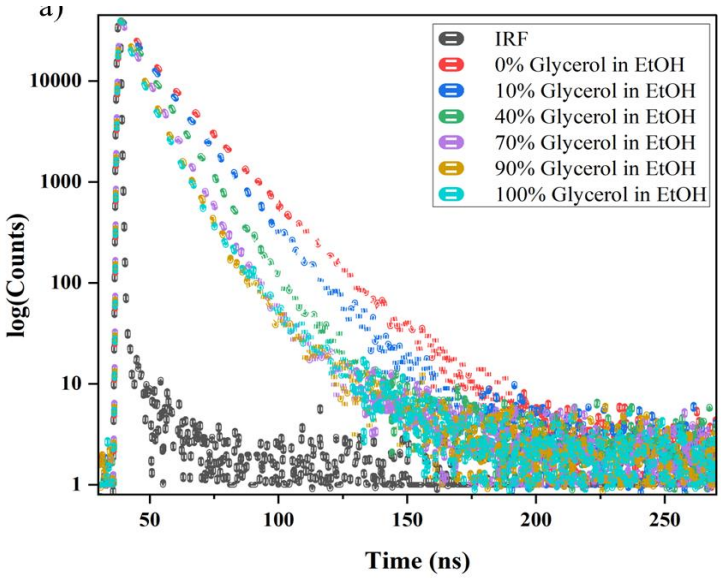

Fig. 23 Lifetime of 3A-NAPH in solvent mixture system

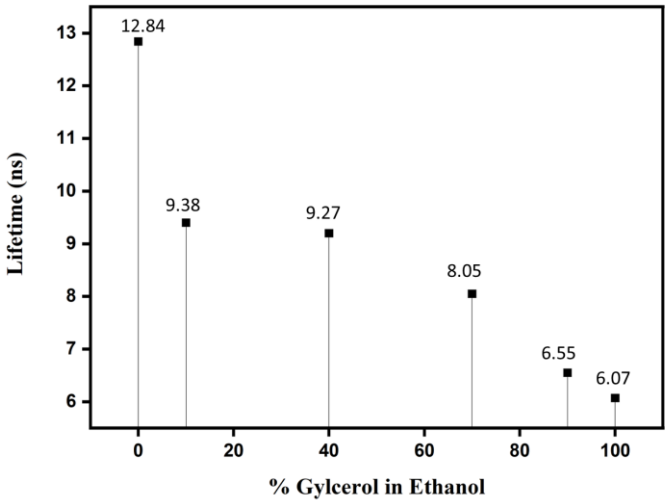

Fig. 24 Lifetime(ns) VS % Glycerol plot of 3A-NAPH

4.3 Solvatochromism study of 3C-NAPH

To study the solvatochromic behavior of our molecule in different solvent polarity order, we take the solvents toluene, chloroform, DCM, ethanol and water. For the Solvatochromism study we make 1mM sample solution in dioxane. The results are discussed below-

4.3.1 Electronic emission study

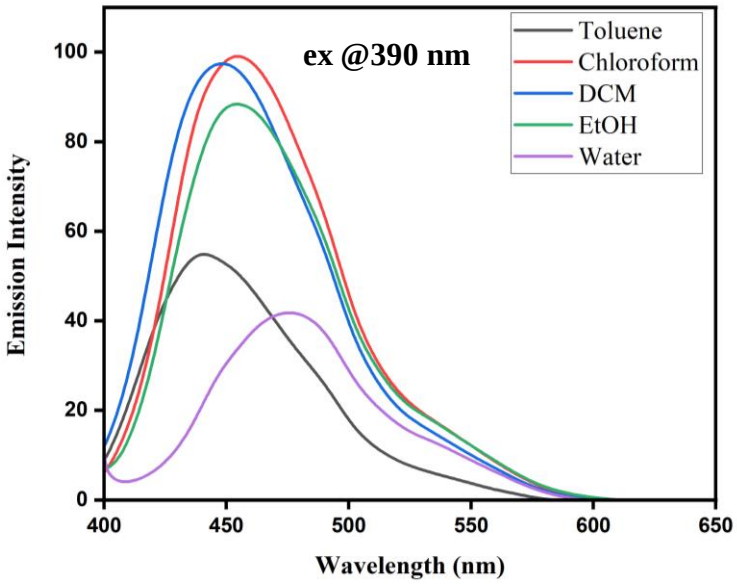

Fig. 25 Emission spectra of 3C-NAPH with different solvent system

The molecule 3C-NAPH is excited at 390 nm and emission spectra is observed and reveals that in toluene—a solvent with low polarity—the emission maximum is found at 441 nm (in arbitrary units). As the solvent polarity increases, a red shift is observed in DCM the maximum moves to 448 nm, in water it shifts further to 477nm, though the intensity drops to 42. This small bathochromic shift indicates that with higher polarity, a locally excited state is being developed, which slightly stabilizes the S_1 state.[24] Also, through Quantum chemical calculations we saw that the electron density is moving towards the chlorobenzene part of the molecule suggesting a better nucleophilic substitution reaction with chlorine, making it a potential GSH sensing probe.

4.4 Concentration dependent study of 3C-NAPH

To study the sensing ability of our molecule in presence of GSH, we first saw the study of probe with GSH with varying concentration of GSH, to find the detection limit. After that to check the amount of probe required to sense 40uM GSH, the study of probe with GSH

with varying concentration of probe has been conducted. All the study for this section is done in 9:1 PBS: DMSO buffer by adding the probe and varying the concentration of GSH and probe. All the study was done after incubating the sample vial for 2.5 hrs. at 40–45-degree Celsius.[9] For the study we make 1mM sample solution of probe in DMSO, and 1mM sample solution of GSH in water. The results are discussed below-

4.4.1 Emission study of probe with GSH with varying concentration of GSH

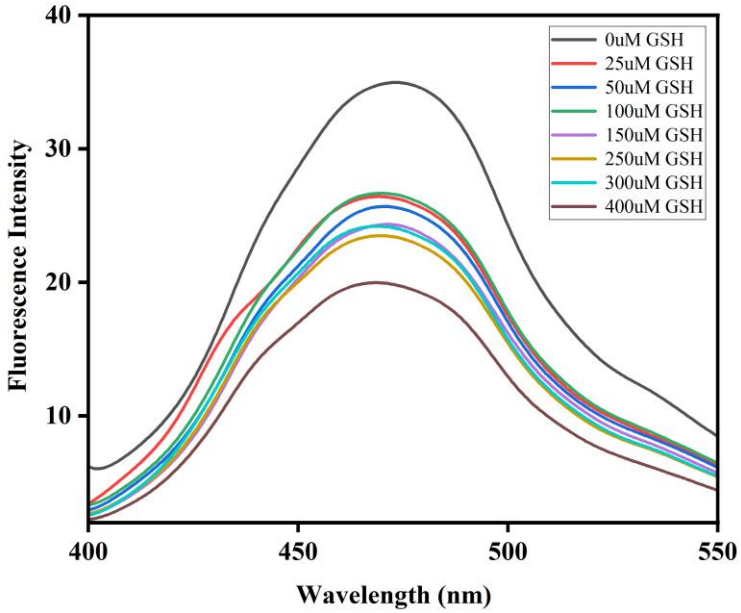

Fig. 26 Emission spectra of 3C-NAPH in different concentration of GSH

The molecule 3C-NAPH with GSH (refer to fig. 11) is excited at 389 nm and emission spectra is observed. It reveals that the emission intensity of probe after showing substitution reaction with GSH shows a decrease in the intensity. This shows that after sensing the GSH the intensity of the probe intensity is reduced and getting reduced on increasing the concentration. The emission maximum is found at 447 nm (in arbitrary units). Also, through Quantum chemical calculations we saw that the electron density is moving towards the chlorobenzene part of the molecule suggesting a change

in electronic configuration possibly leading to the decrease in the intensity. Also in substitution, HCl is formed as a byproduct, which can also be linked with decrease in intensity.

4.4.2 Limit of detection

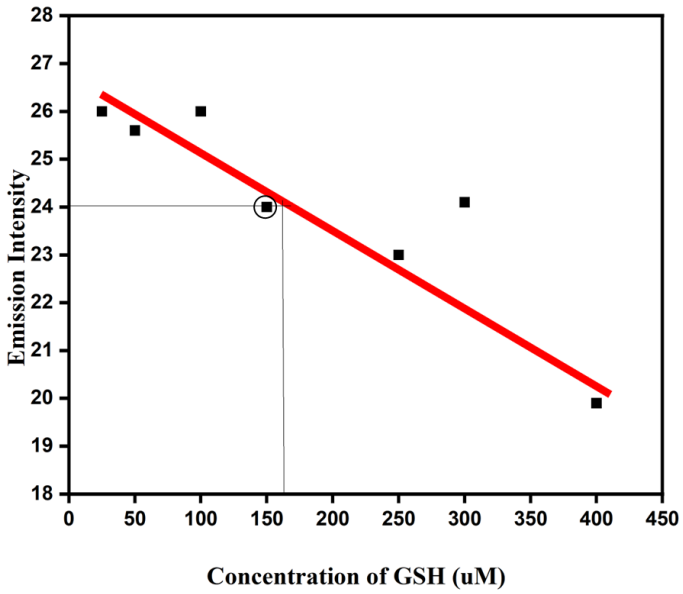

Fig. 27 Plot of emission intensity of 3C-NAPH with different concentration of GSH

In sensing studies, the limit of detection (LOD), which establishes the lowest observable concentration of a material, is crucial. By increasing sensitivity, a lower LOD enables the detection of even trace amounts of analytes.[9] We analyzed and plotted our result and find out the LOD value as 6.53uM. The study was also conducted to find with how much accuracy our probe detects GSH, for that a calibration curve has been plotted for unknown and the error has been found to be 6.6%.

4.4.3 Emission study of probe with GSH with varying concentration of probe

To study about molecule 3C-NAPH with GSH (refer to fig. 11) is excited at 389 nm and emission spectra is observed. It reveals that the emission intensity of probe after showing substitution reaction with GSH shows a decrease in the intensity up to 5uM concentration

after which it increases with increase in probe concentration, showing that for 40uM GSH only 5uM probe is enough to detect. The emission maximum is found at 447 nm (in arbitrary units). We can see a constant behavior till 5uM and after that sudden increase due to increase in probe concentration.

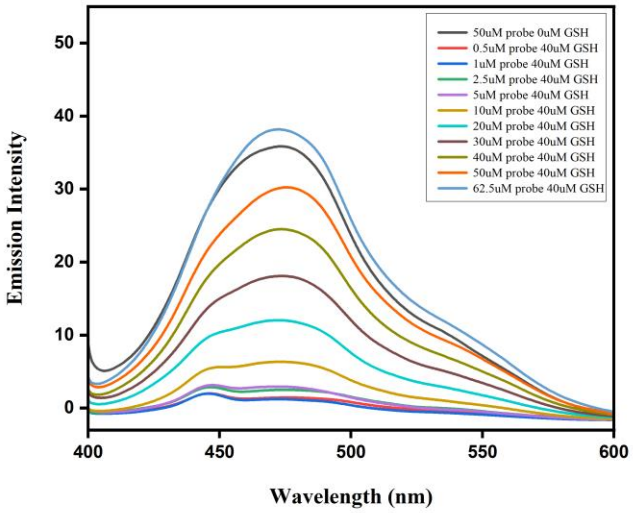

Fig. 28 Emission spectra of different concentration of 3C-NAPH with GSH

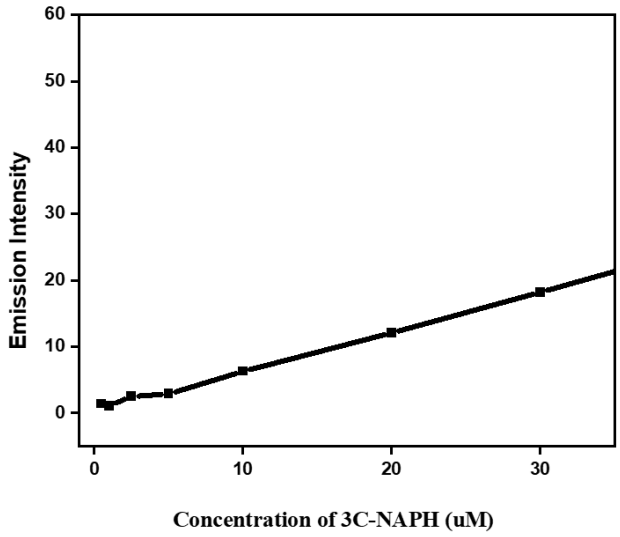

Fig. 29 Plot of emission intensity of different concentration of 3C-NAPH with GSH

4.5 Amino acid dependent study of 3C-NAPH

To study the selective sensing ability of our probe in presence of

GSH, next we saw the study of probe with other amino acids as well like Cysteine, Glycine, GSH and Proline. For competitive study all the amino acids Cysteine, Glycine, GSH and Proline were taken in sample vial with the probe. All the study for this section is done in 9:1 PBS: DMSO buffer and 25uM concentration of amino acids. For the Solvatochromism study we make 1mM sample solution of probe in DMSO, and amino acids in water. The results are discussed below-

4.5.1 Selectivity study of probe

The molecule 3C-NAPH with GSH (refer to fig.11) at 389 nm and other amino acid at 338nm are excited and emission spectra is observed to investigate chemical probe's interaction with bio-thiol and amino acid. It shows a significant intensity relative to other amino acids. It has been concluded that with probe has a selectivity towards GSH.

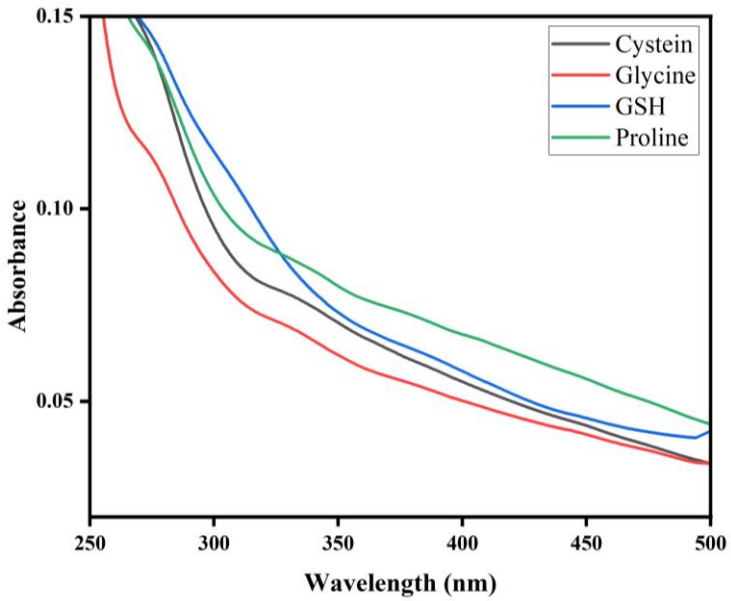

Fig. 30 Absorption spectra of 3C-NAPH with different amino acid and bio-thiol

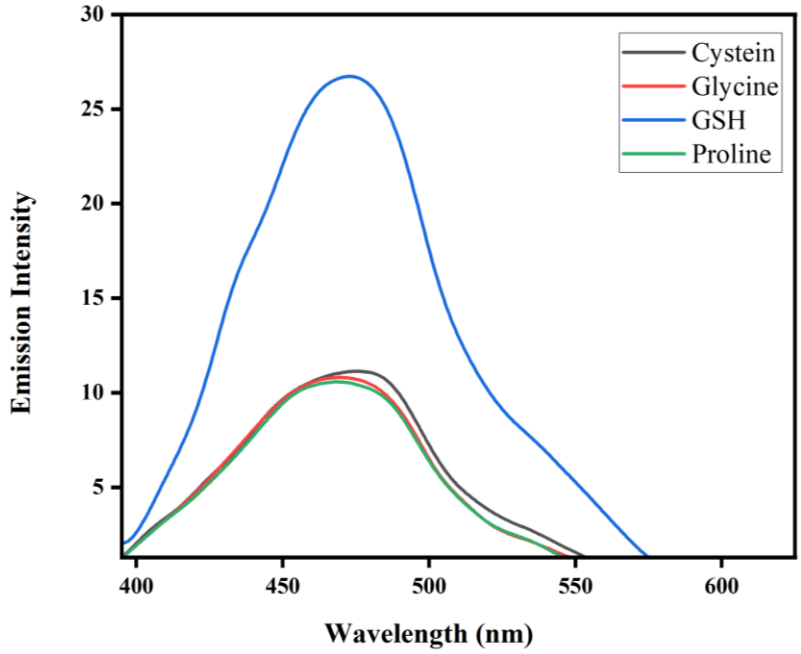

Fig. 31 Emission spectra of 3C-NAPH with different amino acid and bio-thiol

4.5.2 Competitive study of the probe

The sample with all the probe and other amino acids Cysteine, Glycine, GSH and Proline were excited at 389 nm and emission spectra is observed to investigate probe's interaction with bio-thiol and amino acid. It shows a significant spectrum which when compared with probe-GSH spectra, has the same results suggesting that in a competitive environment our probe shows a selectivity with GSH. It has been concluded that with probe has a competitive selectivity towards GSH. With this we can say it as an On-Off sensor.

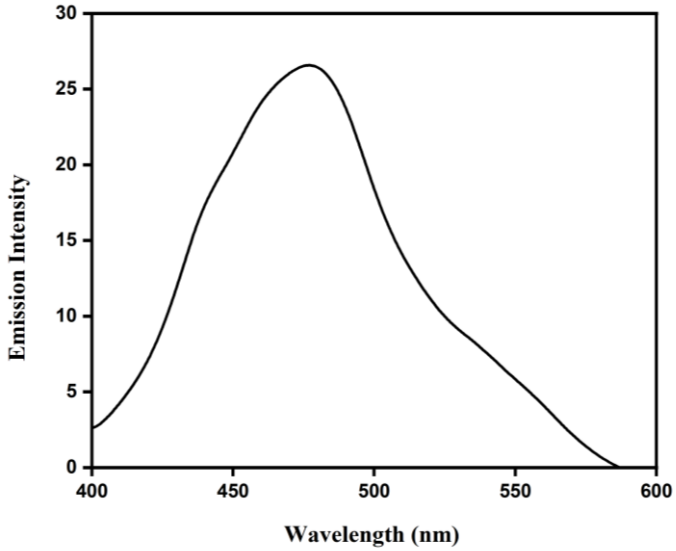

Fig. 32 Emission spectra of 3C-NAPH with amino acid and bio-thiol

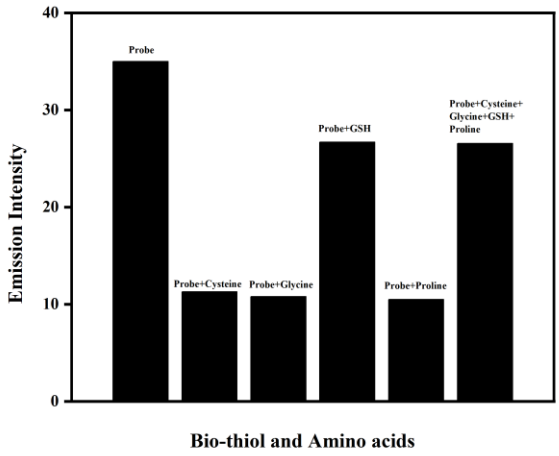

Fig. 33 Plot of emission intensity vs with different amino acid and bio-thiol

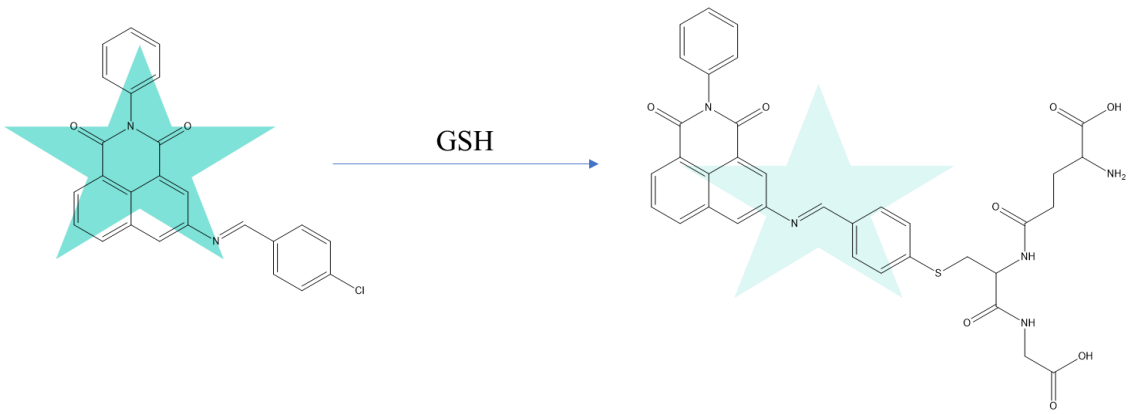

Fig. 34 Diagram to show on-off mechanism of the probe

CHAPTER 5

CONCLUSION AND PROSPECTS

5 CONCLUSION AND PROSPECTS

5.1 Conclusion

In In this research, a novel probe was designed based on the naphthalimide, with expectations of exhibiting sensitive and selective sensing of GSH. The molecule was synthesized via condensation and characterized using IR spectroscopy. A Solvatochromism study revealed a slight red-shifted spectrum and decreased in emission intensity as solvent polarity increased, due to Locally Excited state.

Concentration-dependent emission study showed lower and higher emission intensity at higher concentration of GSH and Probe respectively and the detection limit shows the sensitivity of the probe. Amino acid dependent study suggested the selectivity of probe. The results confirm that the Probe is sensitive, selective and competitive towards GSH.

5.2 Future scope

Future studies could explore the cancer cell imaging and can identify the capability of the probe to detect GSH thereby, detect Cancer cells. Therefore, this can become a promising avenue for cancer screening may arise if GSH is identified early.

CHAPTER 6

REFERENCES

6 REFERENCES

(1) Traverso, N.; Ricciarelli, R.; Nitti, M.; Marengo, B.; Furfaro, A. L.; Pronzato, M. A.; Marinari, U. M.; Domenicotti, C. Role of Glutathione in Cancer Progression and Chemoresistance. *Oxidative Medicine and Cellular Longevity*. 2013. https://doi.org/10.1155/2013/972913.

(2) Gyamfi, J.; Kim, J.; Choi, J. Cancer as a Metabolic Disorder. *International Journal of Molecular Sciences*. MDPI February 1, 2022. https://doi.org/10.3390/ijms23031155.

(3) Gamcsik, M. P.; Kasibhatla, M. S.; Teeter, S. D.; Colvin, O. M. Glutathione Levels in Human Tumors. *Biomarkers*. December 2012, pp 671–691. https://doi.org/10.3109/1354750X.2012.715672.

(4) Zheng, J. Energy Metabolism of Cancer: Glycolysis versus Oxidative Phosphorylation (Review). *Oncology Letters*. December 2012, pp 1151–1157. https://doi.org/10.3892/ol.2012.928.

(5) Liu, G.; Chen, W.; Xu, Z.; Ye, F.; Pan, Y.; Chen, X.; Liu, S. H.; Zeng, L.; Yin, J. Regulating Glutathione-Responsiveness of Naphthalimide-Based Fluorescent Probes by an Oxidation Strategy. *Org Biomol Chem* **2018**, *16* (30), 5517–5523. https://doi.org/10.1039/c8ob01258j.

(6) Kennedy, L.; Sandhu, J. K.; Harper, M. E.; Cuperlovic-culf, M. Role of Glutathione in Cancer: From Mechanisms to Therapies. *Biomolecules*. MDPI AG October 1, 2020, pp 1–27. https://doi.org/10.3390/biom10101429.

(7) Reuter, S.; Gupta, S. C.; Chaturvedi, M. M.; Aggarwal, B. B. Oxidative Stress, Inflammation, and Cancer: How Are They Linked? *Free Radical Biology and Medicine*. December 1, 2010, pp 1603–1616. https://doi.org/10.1016/j.freeradbiomed.2010.09.006.

(8) Bao, X.; Cao, X.; Ai, K.; Cui, Y.; Han, Z.; Zhou, B.; Huo, C. A Dual-Reaction-Site and Dual-Channel Fluorescent-on Probe for Selectively Monitoring Mitochondrial Glutathione. *Sens Actuators B Chem* **2023**, *382*. https://doi.org/10.1016/j.snb.2023.133563.

(9) Cheng, G. J. S.; Qin, J. M.; Li, X.; Cao, Q. Y. A Naphthalimide-Based Fluorescent Probe with Mitochondria Targeting for GSH Sensing and Cancer Cell Recognition.

Dyes and Pigments **2023**, *211*. https://doi.org/10.1016/j.dyepig.2023.111089.

(10) Yadav, A.; Srivastava, S. *Antioxidants and Its Functions in Human Body-A Review*; 2016. https://www.researchgate.net/publication/311674771.

(11) Ketterer, B.; Coles, B.; Meyer, D. J. *The Role of Glutathione in Detoxication*; 1983; Vol. 49.

(12) Ighodaro, O. M.; Akinloye, O. A. First Line Defence Antioxidants-Superoxide Dismutase (SOD), Catalase (CAT) and Glutathione Peroxidase (GPX): Their Fundamental Role in the Entire Antioxidant Defence Grid. *Alexandria Journal of Medicine* **2018**, *54* (4), 287–293. https://doi.org/10.1016/j.ajme.2017.09.001.

(13) Yadav, A.; Srivastava, S. *Antioxidants and Its Functions in Human Body-A Review*; 2016. https://www.researchgate.net/publication/311674771.

(14) Sun, X.; Guo, F.; Ye, Q.; Zhou, J.; Han, J.; Guo, R. Fluorescent Sensing of Glutathione and Related Bio-Applications. *Biosensors*. MDPI January 1, 2023. https://doi.org/10.3390/bios13010016.

(15) Jiang, X.; Chen, J.; Bajić, A.; Zhang, C.; Song, X.; Carroll, S. L.; Cai, Z. L.; Tang, M.; Xue, M.; Cheng, N.; Schaaf, C. P.; Li, F.; MacKenzie, K. R.; Ferreon, A. C. M.; Xia, F.; Wang, M. C.; Maletić-Savatić, M.; Wang, J. Quantitative Real-Time Imaging of Glutathione. *Nat Commun* **2017**, *8*. https://doi.org/10.1038/ncomms16087.

(16) Yan, F.; Zang, Y.; Zhang, Y.; Li, X.; Wang, R.; Lu, Z. The Fluorescent Probe for Detecting Glutathione. *Progress in Chemistry*. Chinese Academy of Sciences May 24, 2022, pp 1136–1152. https://doi.org/10.7536/PC210537.

(17) Yu, H.; Guo, Y.; Zhu, W.; Havener, K.; Zheng, X. Recent Advances in 1,8-Naphthalimide-Based Small-Molecule Fluorescent Probes for Organelles Imaging and Tracking in Living Cells. *Coordination Chemistry Reviews*. Elsevier B.V. October 1, 2021. https://doi.org/10.1016/j.ccr.2021.214019.

(18) Cao, M.; Chen, H.; Chen, D.; Xu, Z.; Liu, S. H.; Chen, X.; Yin, J. Naphthalimide-Based Fluorescent Probe for Selectively and Specifically Detecting Glutathione in the Lysosomes of Living Cells. *Chemical Communications* **2016**, *52* (4), 721–724. https://doi.org/10.1039/c5cc08328a.

(19) Kotowicz, S.; Korzec, M.; Siwy, M.; Golba, S.; Malecki, J. G.; Janeczek, H.; Mackowski, S.; Bednarczyk, K.; Libera, M.; Schab-Balcerzak, E. Novel 1,8-Naphthalimides Substituted at 3-C Position: Synthesis and Evaluation of Thermal,

Electrochemical and Luminescent Properties. *Dyes and Pigments* **2018**, *158*, 65–78. https://doi.org/10.1016/j.dyepig.2018.05.017.

(20) *Preface* K.K. Rohatgi Mukherjee

(21) Lakowicz, J. R. *Principles of Fluorescence Spectroscopy Third Edition*.

(22) Homocianu, M. Exploring Solvatochromism: A Comprehensive Analysis of Research Data. *Microchemical Journal*. Elsevier Inc. March 1, 2024. https://doi.org/10.1016/j.microc.2024.110166.

(23) Kahle, F. J.; Rudnick, A.; Bässler, H.; Köhler, A. How to Interpret Absorption and Fluorescence Spectra of Charge Transfer States in an Organic Solar Cell. *Mater Horiz* **2018**, *5* (5), 837–848. https://doi.org/10.1039/c8mh00564h.

(24) Olsen, S. Locally-Excited (LE) versus Charge-Transfer (CT) Excited State Competition in a Series of Para-Substituted Neutral Green Fluorescent Protein (GFP) Chromophore Models. *Journal of Physical Chemistry B* **2015**, *119* (6), 2566–2575. https://doi.org/10.1021/jp508723d.

(25) Korzec, M.; Kotowicz, S.; Rzycka-Korzec, R.; Schab-Balcerzak, E.; Małecki, J. G.; Czichy, M.; Łapkowski, M. Novel β-Ketoenamines versus Azomethines for Organic Electronics: Characterization of Optical and Electrochemical Properties Supported by Theoretical Studies. *J Mater Sci* **2020**, *55* (9), 3812–3832. https://doi.org/10.1007/s10853-019-04210-3.

(26) Korzec, M.; Malarz, K.; Mrozek-Wilczkiewicz, A.; Rzycka-Korzec, R.; Schab-Balcerzak, E.; Polański, J. Live Cell Imaging by 3-Imino-(2-Phenol)-1,8-Naphthalimides: The Effect of Ex Vivo Hydrolysis. *Spectrochim Acta A Mol Biomol Spectrosc* **2020**, *238*. https://doi.org/10.1016/j.saa.2020.118442.